

## YOUNG STARS IN THE CAMELOPARDALIS DUST AND MOLECULAR CLOUDS. VI. YSOs VERIFIED BY SPITZER AND AKARI INFRARED PHOTOMETRY

V. Straizys and A. Kazlauskas

*Institute of Theoretical Physics and Astronomy, Vilnius University,  
Goštauto 12, Vilnius LT-01108, Lithuania*

Received 2010 April 1; accepted 2010 April 25

**Abstract.** Using photometric data of infrared surveys, young stellar object (YSO) status is verified for 141 objects selected in our previous papers in the Cassiopeia and Camelopardalis segment of the Milky Way bounded by Galactic coordinates  $(\ell, b) = (132\text{--}158^\circ, \pm 12^\circ)$ . The area includes the known star-forming regions in the emission nebulae W3, W4 and W5 and the massive YSO AFGL 490. Spectral energy distribution (SED) curves between 700 nm and 160  $\mu\text{m}$ , constructed from the GSC 2, 2MASS, IRAS, MSX, Spitzer and AKARI data, are used to estimate the evolutionary stages of these stars. We confirm the YSO status for most of the objects. If all of the investigated objects were YSOs, 45% of them should belong to Class I, 41% to class II and 14% to Class III. However, SEDs of some of these objects can be affected by nearby extended infrared sources, like compact H II regions, infrared clusters or dusty galaxies.

**Key words:** stars: formation – stars: pre-main-sequence – infrared: stars – ISM: dust, clouds

### 1. INTRODUCTION

In the previous papers in this series, II and III (Straizys & Laugalys 2007b, 2008a), the Camelopardalis segment of the Milky Way, bounded by Galactic coordinates  $(\ell, b) = (132\text{--}158^\circ, \pm 12^\circ)$ , was shown to be an active region of star formation. Apart from Camelopardalis, the area includes also the neighboring regions of Cassiopeia (with H II regions W3, W4 and W5), Perseus and Auriga. Applying infrared photometry from the 2MASS, IRAS and MSX databases, we identified about 190 objects exhibiting photometric properties of young stellar objects (YSOs). In the present paper, these objects will be called as SL objects. In addition, the area contains more than 40 massive stars of the Cam OB1 association and about 20 young lower-mass stars which exhibit emission in  $\text{H}\alpha$  or belong to a class of irregular variable stars of types IN and IS (Straizys & Laugalys 2007a, Paper I). The region contains a high-mass pre-stellar object, AFGL 490, embedded in the densest part of the dust cloud TGU 942 (Dobashi et al. 2005). According to Zdanavičius et al. (2005) and Straizys & Laugalys (2007a, 2008b), star forming is most active in two layers of dust/molecular clouds at the distances 150–300 pc

and 800–900 pc, which belong to the Gould Belt and the Cam OB1 association, respectively. A large fraction of these objects belong also to the Perseus arm which in this direction is located at a distance of 2.0–2.5 kpc.

In an attempt to verify the YSO status of SL objects, we obtained far-red spectra for 30 brightest objects (Corbally et al. 2008, 2009; Papers IV and V). All of them exhibited emission in  $H\alpha$  line and some also in Ca II and O I lines, in agreement with their pre-main-sequence status. This was also confirmed by infrared spectral energy distributions (SEDs) where observations by IRAS and MSX missions were available.

In 2007–2010, a few papers describing Spitzer observations in the IRAC passbands and 24  $\mu\text{m}$  MIPS passband in star-forming regions (SFRs) of this area were published. Recently, the first two catalogs based on observations in the middle and far infrared from the Japanese AKARI satellite (Murakami et al. 2007) have become available.<sup>1</sup> In the present paper we describe our search of the suspected YSOs in the Spitzer and AKARI data, the construction of their SEDs using the GSC 2, 2MASS, IRAS, MSX, Spitzer and AKARI data, and the estimation of evolutionary stages of the confirmed YSOs.

## 2. IDENTIFICATION OF SL OBJECTS IN THE AKARI, SPITZER AND IRAS CATALOGS

The AKARI data released for public use contain two all-sky catalogs: the IRC Point Source Catalog and the FIS Bright Source Catalog. The first one contains the results of photometry of about 871 000 point sources in two mid-infrared passbands with the mean wavelengths 9  $\mu\text{m}$  and 18  $\mu\text{m}$  (Kataza et al. 2010; Ishihara et al. 2010). The second catalog contains the results of photometry of about 427 000 sources in the far-infrared passbands with the mean wavelengths 65, 90, 140 and 160  $\mu\text{m}$  (Shirahata et al. 2009; Yamamura et al. 2010).

In the AKARI catalogs, we identified 104 SL objects by comparing their equatorial coordinates given in the 2MASS and AKARI catalogs. The search radius around the positions of SL objects (taken from 2MASS) was 10'' for the IRC catalog and 1' for the FIS catalog. In most cases, only one AKARI object was present within the above-mentioned radii around the SL objects. 42 objects were found both in the IRC and FIS catalogs, 28 objects only in IRC and 32 objects only in FIS. Fluxes are available not in all passbands of the IRC and FIS surveys; only reliable fluxes with the quality flag 3 were taken.

The IRAS objects were identified through a search in a 2' radius circle around the SL/2MASS objects using the Vizier facility of the CDS. In some cases the IRAS and 2MASS objects can be different. Such cases will be discussed in Section 4.

Table 1 gives the identifications of SL objects in the 2MASS, IRAS and AKARI IRC and FIS catalogs. The angular distances of the IRAS and AKARI objects from the 2MASS positions are also given.

The Spitzer data for SL objects were taken from the following sources: Gutermuth et al. (2009) for 11 objects in the AFGL 490 SFR, Ruch et al. (2007) for 5 objects in the W3 SFR, Koenig et al. (2008) for 21 objects in the W5 SFR and Kumar Dewangan & Anandarao (2010) for one object in the AFGL 437 SFR.

---

<sup>1</sup> <http://www.ir.isas.jaxa.jp/AKARI/Observation/PSC/Public/>

**Table 1.** Identification of the SL objects in the 2MASS, IRAS and AKARI catalogs having mid- and far-infrared measurements. The objects without IRAS and AKARI numbers have been measured only by Spitzer and MSX. Nine known YSOs in the same area are listed at the end of the Table. Separations between the 2MASS and the IRAS and AKARI objects are given in arcseconds.

ID	2MASS	IRAS	Sep.	AKARI-IRC-V1	Sep.	AKARI-FIS-V1	Sep.
SL 1	J02115015+6239356	02081+6225	5.3	J0211497+623941	6.8	J0211493+623952	17.6
SL 3	J02413774+6947098	02371+6934	1.2	J0241377+694708	1.0	J0241387+694707	5.7
SL 4	J02444712+6959571	02402+6947	9.3	J0244472+695957	0.8		
SL 5	J02474082+6933066	02432+6919	91.5				
SL 6	J02465383+6906314			J0246539+690632	0.7		
SL 7	J02165920+6108158	02134+6053	103.2			J0217020+610836	28.0
SL 8	J02513724+6914018	02470+6901	14.2				
SL 9	J02202209+6132219	02167+6118	24.8	J0220220+613221	0.6	J0220240+613155	29.8
SL 10	J02192184+6107069	02157+6053	21.7	J0219216+610707	1.1	J0219252+610721	28.3
SL 11	J02210026+6128560	02173+6113	116.2				
SL 13	J02230386+6205135					J0223013+620445	34.0
SL 14	J02541453+6918367						
SL 15	J02230616+6158437			J0223061+615843	0.2		
SL 16	J02210449+6106045	02174+6052	29.7	J0221044+610604	0.6	J0221063+610602	13.1
SL 18	J02245191+6209367					J0224555+620941	25.6
SL 20	J02250325+6159477						
SL 21	J02231856+6125416			J0223185+612541	0.3		
SL 23	J02253880+6207297					J0225340+620701	44.2
SL 25	J02255757+6211497					J0225598+621159	18.2
SL 27	J02254436+6206117	02219+6152	13.0	J0225442+620616	5.3	J0225467+620626	22.1
SL 30	J02253198+6157249						
SL 31	J02262447+6210384						
SL 34	J02262572+6203559	02226+6150	5.7	J0226254+620353	2.8		
SL 35	J02265368+6212000	02230+6157	81.0			J0226509+621218	26.5
SL 36	J02263669+6153085					J0226313+615306	38.0
SL 37	J02271602+6200506			J0227172+620053	8.8	J0227184+620030	26.8
SL 38	J02254737+6120562	02220+6107	9.6	J0225475+612056	1.4	J0225481+612057	5.4
SL 39	J02264501+6129430			J0226452+612942	1.5	J0226467+612933	15.8
SL 40	J02271217+6137055			J0227115+613702	5.7	J0227112+613726	21.1

Table 1. Continued

ID	2MASS	IRAS	Sep.	AKARI-IRC-V1	Sep.	AKARI-FIS-V1	Sep.
SL 41	J02252125+6057581	02215+6044	21.1	J0225210+605758	1.8	J0225200+605809	14.0
SL 43	J02282010+6130351	02244+6117	56.8				
SL 44	J02282148+6128369	02245+6115	7.9			J0228217+612856	19.3
SL 48	J02363576+6031518	02327+6019	24.8	J0236354+603153	2.9	J0236341+603214	25.7
SL 49	J02512318+6209031	02475+6156	75.4	J0251228+620903	2.5	J0251303+620847	52.3
SL 50	J02470551+6102451	02431+6050	5.9	J0247053+610245	1.5	J0247059+610249	5.0
SL 51	J02460197+6039438					J0246010+604031	48.2
SL 52	J02482571+6055051	02445+6042	4.5	J0248255+605506	1.8	J0248248+605508	6.8
SL 53	J02485350+6045115						
SL 54	J02492991+6047287	02455+6034	56.2	J0249297+604728	0.9		
SL 55	J02492190+6045041						
SL 56	J02494739+6042090	02459+6029	2.6	J0249472+604208	1.1	J0249447+604238	34.7
SL 57	J02502403+6036287	02465+6024	27.8				
SL 58	J02590280+6225295			J0259026+622530	1.6		
SL 59	J02512557+6006048						
SL 60	J02513283+6003542	02476+5950	49.5	J0251328+600353	0.7	J0251330+600341	13.0
SL 61	J02551296+6042404			J0255129+604241	0.6	J0255116+604258	20.7
SL 62	J02572154+6053097	02532+6042	106.9	J0257214+605309	1.1	J0257225+605314	8.2
SL 63	J02572160+6041198	02534+6029	28.0			J0257171+604203	54.2
SL 64	J02573189+6038171	02533+6026	103.5			J0257323+603829	12.6
SL 65	J03001592+6059240	02563+6047	33.2	J0300158+605924	0.6	J0300155+605934	10.6
SL 66	J03013187+6029256	02575+6017	14.3			J0301314+602926	3.9
SL 68	J03113336+6222086	03074+6211	51.5				
SL 69	J03025804+6027571						
SL 70	J03031387+6028092						
SL 71	J03032084+6029284			J0303209+602928	0.7		
SL 72	J03031615+6027502	02593+6016	12.7				
SL 74	J03051264+6048430			J0305124+604844	2.0	J0305110+604915	34.0
SL 75	J03032586+6023095	02595+6011	27.7	J0303257+602309	1.3		
SL 77	J02512410+5542038	02476+5529	72.2			J0251208+554217	30.7
SL 78	J02514696+5542014			J0251469+554202	1.3	J0251409+554223	55.8
SL 79	J03104626+5930035	03068+5918	21.7	J0310461+593003	1.0		

Table 1. Continued

ID	2MASS	IRAS	Sep.	AKARI-IRC-V1	Sep.	AKARI-FIS-V1	Sep.
SL 80	J03072452+5830433	03035+5819	12.2	J0307241+583047	5.1	J0307233+583112	30.2
SL 81	J03153845+6002404	03116+5951	14.0	J0315382+600241	1.4		
SL 82	J03172590+6009417	03134+5958	5.6	J0317258+600942	0.8	J0317256+600944	3.1
SL 83	J03152500+5855482	03114+5844	9.9	J0315249+585548	0.4	J0315254+585557	9.4
SL 84	J03153715+5857208					J0315306+585712	51.2
SL 85	J03300237+6125473			J0330022+612547	0.8		
SL 86	J03130254+5804483	03091+5753	11.1	J0313026+580449	1.3	J0313029+580443	5.8
SL 87	J03084929+5649572	03050+5638	12.8	J0308489+564957	2.9	J0308480+565001	11.2
SL 88	J03081580+5623388	03045+5612	15.7			J0308185+562340	22.7
SL 89	J03264934+5845238	03228+5834	6.4	J0326493+584525	1.2	J0326475+584524	14.5
SL 91	J03265964+5842199						
SL 93	J03271645+5844376	03233+5833	79.0	J0327175+584440	9.2		
SL 94	J03273489+5847485						
SL 95	J03273876+5847000	03236+5836	2.6	J0327386+584700	0.7		
SL 96	J03271170+5840269			J0327114+584028	2.4	J0327157+583959	41.8
SL 97	J03280189+5847091						
SL 98	J03274898+5812164			J0327489+581218	1.7		
SL 100	J03310105+5803448					J0330594+580354	16.3
SL 101	J03290756+5701336			J0329074+570133	0.6		
SL 102	J03330101+5734127	03290+5724	13.4	J0333009+573416	3.4	J0333018+573412	6.4
SL 104	J03224839+5503371	03188+5452	82.9				
SL 106	J03235137+5452434	03201+5442	33.2	J0323516+545240	3.7		
SL 107	J03341497+5653213	03303+5643	18.1				
SL 108	J03250185+5456160	03211+5446	72.5				
SL 109	J03331001+5510549	03293+5500	3.6	J0333098+551054	1.1	J0333100+551054	1.4
SL 110	J03323036+5450449	03286+5440	8.5			J0332296+545051	8.8
SL 111	J03364225+5447431	03328+5437	11.2	J0336423+544743	0.8		
SL 112	J03390466+5345239	03353+5333	148.1	J0339047+534524	0.8		
SL 113	J03484016+5432136	03447+5422	27.5			J0348418+543158	21.4
SL 115	J03554277+5350074	03518+5341	26.6	J0355425+535007	2.2		
SL 116	J03553004+5345419	03516+5336	17.3	J0355299+534542	0.8	J0355278+534520	29.5
SL 118	J04082550+5508284	04044+5500	19.1	J0408254+550829	1.0	J0408260+550834	6.9

Table 1. Continued

ID	2MASS	IRAS	Sep.	AKARI-IRC-V1	Sep.	AKARI-FIS-V1	Sep.
SL 120	J04075001+5441157	04038+5433	39.2	J0407497+544116	2.5	J0407499+544129	13.1
SL 121	J04192876+5418579			J0419287+541857	0.8		
SL 123	J04034287+5123423			J0403428+512343	0.8		
SL 124	J04044961+5126572	04010+5118	23.4	J0404496+512657	0.2	J0404500+512658	3.7
SL 125	J04145692+5220313	04110+5212	11.9			J0414574+522036	6.2
SL 126	J04193181+5251221	04156+5244	10.3	J0419326+525121	7.7	J0419329+525122	10.0
SL 129	J04111220+5110238	04073+5102	63.1				
SL 130	J04101185+5059544	04064+5052	3.5	J0410118+505954	0.3	J0410117+505942	12.2
SL 131	J04071005+5018240	04034+5010	4.5	J0407100+501823	0.1	J0407097+501824	3.5
SL 132	J04083557+5031588			J0408356+503158	0.3		
SL 133	J04154142+4915218	04119+4907	5.3			J0415418+491509	13.4
SL 134	J04232978+4919314	04198+4912	36.8			J0423303+491923	10.3
SL 135	J04344416+5039275	04308+5033	23.7			J0434442+503945	17.3
SL 137	J04271337+4804149	04235+4757	2.9	J0427135+480415	1.8	J0427128+480419	6.7
SL 138	J04264419+4642295	04230+4635	30.2			J0426444+464200	29.2
SL 140	J04254952+4604387	04222+4557	27.0			J0425502+460431	10.4
SL 141	J04204895+4417280	04172+4411	82.2				
SL 142	J04022981+4042418	03591+4034	10.3	J0402298+404241	0.2		
SL 143	J03262717+5848241					J0326263+584818	8.9
SL 145	J03270030+5846164						
SL 146	J03270077+5844307						
SL 147	J03265892+5842531						
SL 148	J03272257+5843170	03233+5833	23.4			J0327253+584336	28.1
SL 149	J03280190+5847030						
SL 155	J03273738+5803381	03238+5752	79.1				
SL 158	J03300545+5813253	03261+5803	1.0	J0330054+581325	0.4	J0330052+581327	2.9
SL 159	J03295426+5805396	03260+5755	60.3				
SL 160	J03285987+5753402					J0329039+575302	49.6
SL 162	J03312962+5816425					J0331284+581716	35.3
SL 163	J03325315+5827511	03289+5818	91.0				
SL 165	J03340073+5816376			J0334004+581637	2.0		
SL 169	J03333964+5809204	03298+5758	84.7				

Table 1. Continued

ID	2MASS	IRAS	Sep.	AKARI-IRC-V1	Sep.	AKARI-FIS-V1	Sep.
SL 171	J03313040+5721567			J0331302+572157	1.6		
SL 172	J03334575+5732396	03296+5723	85.2				
SL 174	J03300550+5547529	03262+5536	80.9				
SL 175	J03205334+5849395	03167+5840	101.4	J0320530+584940	2.4	J0320529+584947	8.3
SL 176	J03172447+5754136	03135+5743	5.3	J0317244+575412	1.1		
SL 177	J03275850+5858341	03239+5849	60.4				
SL 178	J03235621+5804391	03199+5755	90.0				
SL 179	J03233167+5757520	03194+5746	84.7				
SL 180	J03251924+5811455	03213+5801	22.0	J0325191+581146	1.2		
SL 181	J03300680+5826389	03263+5816	91.6			J0330097+582727	53.3
SL 182	J03265911+5740027	03231+5730	78.5			J0326583+573959	7.0
SL 183	J03284786+5755560	03248+5745	2.6	J0328479+575557	1.0	J0328478+575552	4.0
SL 184	J03300294+5805348	03260+5755	9.2	J0330027+580535	1.6		
SL 185	J03312047+5805488	03275+5755	94.2			J0331217+580626	38.8
SL 186	J03330645+5817165	03292+5806	47.3				
SL 187	J03354115+5725589	03317+5716	53.3				

Table 1. Continued

ID	2MASS	IRAS	Sep.	AKARI-IRC-V1	Sep.	AKARI-FIS-V1	Sep.
KW97 14-24	J03012159+6028566	02575+6017	80.5				
KW97 14-52	J03082443+5943265			J0308244+594326	0.4		
IRAS 03243+5819	J03281460+5829374	03243+5819	18.4	J0328144+582938	1.3		
LkH $\alpha$ 272	J03490512+3856172	03456+3846	72.9	J0349050+385617	0.8		
XY Per	J03493638+3858556	03462+3849	2.8	J0349363+385855	0.1	J0349363+385902	6.0
Gahm 21	J03595342+5131463	03561+5123	30.9				
KW97 16-55	J04011993+5311221	03573+5302	100.2				
OS Per	J04362931+4916207	04325+4911	113.0				
V347 Aur	J04565702+5130509	04530+5126	2.2	J0456570+513050	0.4	J0456569+513050	1.1

### 3. SPECTRAL ENERGY DISTRIBUTIONS

For the identified SL objects a table with reliable fluxes from the 2MASS, IRAS, MSX, Spitzer and AKARI surveys was compiled. The data in the table were supplemented by the photographic red  $F$  magnitudes extracted from the GSC 2.3.2 catalog available at the CDS (Lasker et al. 2008). The IRAS, MSX and AKARI fluxes in Janskys were transformed simply to  $\log \lambda F_\lambda$ . The  $F$  and 2MASS magnitudes were transformed to  $\log \lambda F_\lambda$  by the equations given in Paper II (p. 341–342), accepting that the magnitudes  $F = R$  and using for them the absolute calibration from Straizys (1992).

The Vega fluxes in Janskys, used in the transformation of the Spitzer magnitudes to fluxes, were taken from Reach et al. (2005) for the IRAC data and from Rieke et al. (2008) for the 24  $\mu\text{m}$  MIPS data:

$$[3.6] = -2.5 \log (F[Jy]/280.9), \quad (1)$$

$$[4.5] = -2.5 \log (F[Jy]/179.7), \quad (2)$$

$$[5.8] = -2.5 \log (F[Jy]/115.0), \quad (3)$$

$$[8.0] = -2.5 \log (F[Jy]/64.1), \quad (4)$$

$$[24.0] = -2.5 \log (F[Jy]/7.15). \quad (5)$$

The resulting values of  $\log \lambda F_\lambda$  for 141 SL objects are given in Tables 2 and 3: the first one contains 127 objects for which the data from IRAS, MSX or AKARI surveys are available, and the second one contains 37 objects identified in the Spitzer catalogs. At the end of Table 2 the data for nine known YSOs in the same area, discussed in Papers I and IV, are added. The plots of  $\log \lambda F_\lambda$  vs.  $\log \lambda$  for the 141 SL objects and nine known YSOs are shown in Figure 1.

The traditional classification scheme of YSOs (Lada 1987) is based on their SEDs longward of 2  $\mu\text{m}$ . The spectral index

$$a = \frac{d \log (\lambda F_\lambda)}{d \log \lambda} \quad (6)$$

for Class I objects is positive, for Class II objects it is close to zero or slightly negative and for Class III objects it is negative. Evolutionary interpretation of SEDs has been given by Whitney et al. (2003a,b, 2004) and Robitaille et al. (2006, 2007) using tens of thousands of YSO models with disks and envelopes.

Examination of our  $\log \lambda F_\lambda$  vs.  $\log \lambda$  plots indicates that SEDs longward of 2  $\mu\text{m}$  for 45% of the objects show increase in intensity, for 41% of the objects SEDs remain more or less at the same level and for 14% of the objects SEDs exhibit a tendency to decrease. If all of these objects were YSOs, then we should conclude that the majority of them are young stars either embedded into dense gas and dust envelopes which reradiate energy of the central source (Class I) or have optically thick disks and possible remains of tenuous infalling envelopes (Class II, T Tauri and Herbig Ae/Be stars). Only a small fraction of the objects with the SEDs with a negative spectral index should belong to Stage III (or post T Tauri-type) objects with thin disks and weak emission lines. These objects hardly can be normal heavily reddened stars since SEDs of such stars exhibit much steeper negative slope (see Paper II, Figure 5).



**Table 2.** The values of  $\log \lambda F_\lambda$  for the suspected YSOs in the passbands of the 2MASS, IRAS, MSX and AKARI surveys.  $F$  are red photographic magnitudes from the GSC 2.3.2 catalog.

SL	$F$	$J$	$H$	$K$	IRAS [12]	IRAS [25]	IRAS [60]	IRAS [100]	MSX [8.3]	AKARI [9]	AKARI [18]	AKARI [65]	AKARI [90]	AKARI [140]	AKARI [160]
1	-12.137	-11.202	-10.932	-10.821	-10.058	-10.088	-9.623	-9.496	-	-9.986	-10.139	-9.824	-9.606	-9.454	-9.606
3	-12.277	-11.394	-10.928	-10.657	-	-10.541	-	-	-	-10.282	-10.426	-	-10.625	-	-
4	-12.197	-10.834	-10.388	-10.241	-	-10.523	-10.678	-	-	-10.419	-10.390	-	-	-	-
5	-11.853	-11.194	-10.792	-10.729	-	-	-10.561	-	-	-	-	-	-	-	-
6	-12.369	-11.294	-10.900	-10.637	-	-	-	-	-	-10.207	-	-	-	-	-
7	-12.933	-11.458	-11.068	-10.857	-	-	-	-9.313	-	-	-	-	-10.309	-	-
8	-12.349	-11.210	-10.704	-10.533	-	-10.115	-10.171	-9.653	-	-	-	-	-10.318	-9.910	-
9	-11.373	-10.614	-10.456	-10.393	-	-10.319	-9.771	-	-	-10.121	-10.311	-	-9.763	-9.353	-9.765
10	-	-11.162	-10.660	-10.465	-9.688	-9.804	-8.963	-	-	-10.080	-10.203	-9.321	-9.089	-9.252	-9.384
11	-12.721	-11.214	-10.752	-10.561	-10.097	-9.921	-9.456	-	-	-	-	-	-	-	-
13	-12.461	-11.318	-11.068	-10.989	-	-	-	-	-	-	-	-	-	-9.894	-
14	-12.893	-11.234	-10.812	-10.649	-	-	-	-	-10.266	-	-	-	-	-	-
15	-12.729	-10.986	-10.544	-10.489	-	-	-	-	-	-10.378	-10.354	-	-	-	-
16	-	-11.570	-10.952	-10.577	-9.658	-9.548	-	-	-	-10.129	-10.042	-9.572	-9.594	-9.310	-9.404
18	-12.085	-11.038	-10.764	-10.689	-	-	-	-	-	-	-	-8.449	-8.843	-8.377	-8.139
21	-10.985	-10.442	-10.156	-10.037	-	-	-	-	-	-10.158	-10.363	-	-	-	-
23	-	-10.562	-10.128	-9.897	-	-	-	-	-	-	-	-6.694	-7.107	-6.947	-6.695
25	-12.645	-11.114	-10.800	-10.701	-	-	-	-	-	-	-	-	-8.487	-8.485	-8.266
27	-	-10.242	-9.712	-9.585	-6.759	-6.188	-	-5.899	-	-6.923	-	-6.748	-	-6.975	-
34	-	-9.866	-9.020	-8.741	-9.305	-	-	-	-	-9.391	-	-	-	-	-
35	-	-11.126	-10.776	-10.689	-9.326	-	-	-	-	-	-	-	-	-8.769	-8.492
36	-	-11.502	-10.872	-10.689	-	-	-	-	-	-	-	-8.476	-8.750	-8.491	-8.447
37	-10.253	-9.298	-9.136	-9.081	-	-	-	-	-	-8.963	-	-8.151	-	-8.666	-
38	-	-11.530	-10.940	-10.761	-9.745	-9.486	-9.186	-8.834	-	-10.447	-9.825	-9.433	-9.351	-9.383	-9.386
39	-12.773	-11.110	-10.740	-10.685	-	-	-	-	-	-10.600	-10.286	-	-9.570	-	-
40	-	-10.594	-10.300	-10.245	-	-	-	-	-	-9.420	-	-8.936	-	-	-9.129
41	-12.301	-11.194	-10.880	-10.797	-9.839	-9.986	-9.871	-9.402	-	-10.213	-10.207	-	-10.207	-9.948	-
43	-	-11.126	-10.724	-10.669	-8.650	-	-	-7.442	-	-	-	-	-	-	-
44	-	-10.890	-10.264	-10.049	-8.474	-8.338	-7.520	-	-	-	-	-7.631	-7.816	-7.972	-7.951
48	-	-10.614	-10.272	-10.149	-9.206	-9.423	-8.689	-8.404	-	-9.211	-9.819	-8.684	-8.750	-8.752	-8.792
49	-11.477	-10.782	-10.364	-10.153	-9.498	-	-	-	-	-9.518	-9.745	-9.175	-9.161	-9.387	-9.320
50	-12.645	-11.270	-10.592	-10.205	-9.727	-9.018	-	-	-	-9.709	-9.582	-9.798	-9.896	-9.731	-
51	-12.421	-11.314	-10.968	-10.897	-	-	-	-	-	-	-	-	-10.076	-9.723	-
52	-	-11.102	-9.960	-9.401	-8.835	-8.883	-8.687	-8.745	-	-8.831	-8.954	-8.635	-8.880	-8.980	-8.904
54	-11.809	-9.870	-9.276	-8.945	-8.888	-8.533	-8.075	-	-	-8.864	-8.728	-	-	-	-

Table 2. Continued

SL	$F$	$J$	$H$	$K$	IRAS [12]	IRAS [25]	IRAS [60]	IRAS [100]	MSX [8.3]	AKARI [9]	AKARI [18]	AKARI [65]	AKARI [90]	AKARI [140]	AKARI [160]
56	—	-10.518	-9.372	-8.669	-8.206	-8.110	-8.051	—	—	-8.096	-8.161	-8.358	-8.497	-8.436	-8.162
57	-12.869	-11.222	-10.920	-10.845	-9.870	—	—	—	—	—	—	—	—	—	—
58	-12.057	-11.174	-10.776	-10.673	—	—	—	—	—	-10.520	—	—	—	—	—
60	-11.717	-10.618	-10.304	-10.229	-9.854	—	—	—	—	-10.180	-10.063	-9.467	-9.451	-9.319	-9.343
61	—	-11.170	-10.460	-10.141	—	—	—	—	—	-9.804	-9.935	-9.398	-9.278	-9.184	-9.284
62	-12.557	-11.046	-10.820	-10.761	-9.721	-9.444	-9.824	—	—	-10.054	-9.857	—	-9.820	—	—
63	-11.493	-10.414	-10.132	-10.061	—	-9.565	—	—	—	—	—	—	—	—	—
64	-12.945	-10.938	-10.512	-10.385	-8.742	-9.013	-8.102	—	—	—	—	—	-8.729	—	—
65	-12.381	-11.314	-10.872	-10.685	—	-10.365	—	-8.811	—	-10.286	-10.380	-9.960	-9.751	—	-9.272
66	—	-11.578	-10.864	-10.601	-8.303	-7.594	-7.416	-7.489	—	—	—	—	—	-7.675	-7.601
68	—	-11.026	-10.940	-10.849	—	—	—	-9.874	—	—	—	—	—	—	—
71	—	-11.110	-10.916	-10.789	—	—	—	—	—	-9.049	—	—	—	—	—
72	—	-11.138	-10.372	-10.145	-8.429	-8.008	-7.264	-7.201	—	—	—	—	—	—	—
74	-12.501	-11.230	-10.832	-10.745	—	—	—	—	—	—	-10.619	—	-10.554	-9.789	—
75	-10.601	-10.086	-9.720	-9.581	-9.553	-9.680	—	—	—	-9.615	-9.749	—	—	—	—
77	-11.625	-11.406	-11.056	-10.893	—	-10.402	-9.602	—	—	—	—	—	-10.167	-10.046	—
78	-10.169	-9.878	-9.728	-9.657	—	—	—	—	-10.163	-10.124	-10.662	—	-10.724	-10.348	—
79	-10.977	-10.546	-10.396	-10.309	-10.187	-10.287	—	—	—	-10.187	-10.564	—	—	—	—
80	—	-10.522	-10.048	-9.857	-8.111	-7.323	-7.276	-7.409	—	-8.132	-7.448	-7.256	—	-8.056	-8.019
81	-12.897	-10.994	-10.544	-10.425	-10.011	-10.188	—	-9.077	-10.266	-10.040	-10.168	—	—	—	—
82	-8.653	-9.274	-9.024	-8.957	-9.321	-9.599	-9.331	-8.953	-9.315	-9.350	-9.628	-9.438	-9.288	-9.345	-9.401
83	-12.553	-10.806	-10.196	-9.929	-9.939	-9.800	-9.590	—	—	-9.827	-9.824	—	-9.898	-9.746	—
84	-11.813	-11.326	-11.084	-11.001	—	—	—	—	—	—	—	—	-9.801	-9.991	-9.981
85	-10.665	-10.602	-10.392	-10.329	—	—	—	—	—	-10.413	—	—	—	—	—
86	-12.493	-10.470	-10.008	-9.905	—	-10.268	-10.310	—	—	-10.338	-10.389	—	-10.300	-9.711	-9.996
87	—	-10.570	-10.308	-10.261	-9.516	-9.908	-8.933	-8.476	—	-9.271	—	-8.885	-8.995	-8.963	-9.118
88	-11.897	-10.930	-10.608	-10.505	-9.290	-9.211	-9.354	-9.206	—	—	—	-9.586	-9.589	-9.506	—
89	-12.593	-10.838	-10.460	-10.409	-10.222	-9.896	—	—	—	-10.346	-9.966	—	-9.798	-9.379	—
93	—	-11.442	-10.904	-10.793	—	-9.853	—	—	—	-10.451	—	—	—	—	—
95	-11.997	-9.798	-8.928	-8.337	-7.645	-7.458	-7.447	-7.460	-7.704	-7.785	-7.558	—	—	—	—
96	—	-11.394	-10.892	-10.753	—	—	—	—	—	—	-10.729	—	-9.955	—	—
98	-12.133	-10.698	-10.448	-10.357	—	—	—	—	—	-10.254	—	—	—	—	—
100	-12.045	-10.906	-10.520	-10.413	—	—	—	—	—	—	—	—	-10.399	-9.761	-9.614
101	-10.889	-10.102	-10.004	-9.957	—	—	—	—	-10.401	-10.233	—	—	—	—	—
102	-12.449	-10.958	-10.640	-10.553	—	-10.690	—	—	—	—	-10.448	—	-10.370	-9.910	—
104	-12.585	-11.298	-11.004	-10.897	—	-9.967	-10.301	-9.350	<i>inf</i>	—	—	—	—	—	—
106	-11.177	-10.774	-10.396	-10.273	-10.125	-10.222	—	—	—	-9.844	-10.158	—	—	—	—



Table 2. Continued

SL	<i>F</i>	<i>J</i>	<i>H</i>	<i>K</i>	IRAS [12]	IRAS [25]	IRAS [60]	IRAS [100]	MSX [8.3]	AKARI [9]	AKARI [18]	AKARI [65]	AKARI [90]	AKARI [140]	AKARI [160]
165	-11.089	-10.282	-10.092	-10.089	—	—	—	—	-10.296	-10.297	-10.564	—	—	—	—
169	-12.417	-11.258	-10.960	-10.997	-10.000	-10.150	-9.500	-9.094	—	—	—	—	—	—	—
171	-11.569	-9.430	-9.028	-8.997	—	—	—	—	-9.851	-9.960	—	—	—	—	—
172	-12.377	-11.318	-11.152	-11.193	-10.140	-9.143	-9.347	—	—	—	—	—	—	—	—
174	-12.789	-11.554	-11.380	-11.397	—	—	-10.240	-9.601	—	—	—	—	—	—	—
175	-10.301	-10.106	-10.188	-10.329	-9.727	-10.389	-10.122	—	—	-10.480	—	—	-10.559	—	—
176	-10.725	-10.378	-10.360	-10.465	—	-10.620	—	—	—	—	-10.604	—	—	—	—
177	-11.481	-10.682	-10.548	-10.625	—	—	-9.528	—	—	—	—	—	—	—	—
178	-12.893	-11.298	-11.156	-11.257	—	—	—	-9.317	—	—	—	—	—	—	—
179	—	-11.570	-11.480	-11.589	—	—	-10.382	—	—	—	—	—	—	—	—
180	-10.953	-10.238	-10.172	-10.229	—	-10.389	—	—	—	-10.318	-10.357	—	—	—	—
181	-12.837	-11.506	-11.424	-11.533	—	—	-10.190	—	—	—	—	—	—	-9.740	—
182	-13.069	-11.538	-11.420	-11.521	—	—	-10.545	-9.563	—	—	—	—	-10.666	—	—
183	-10.537	-10.362	-10.420	-10.537	-10.111	-9.939	—	—	—	-10.116	-10.028	—	-10.775	—	—
184	-11.841	-10.626	-10.416	-10.493	—	-10.523	—	—	—	-10.537	-10.838	—	—	—	—
185	-13.129	-11.438	-11.292	-11.389	—	—	—	-9.596	—	—	—	—	-10.708	-9.986	—
186	-12.373	-11.238	-11.048	-11.125	—	-10.287	—	-9.498	—	—	—	—	—	—	—
187	-12.261	-11.078	-10.996	-11.149	—	—	-10.530	—	—	—	—	—	—	—	—

Table 2. Continued

ID	<i>F</i>	<i>J</i>	<i>H</i>	<i>K</i>	IRAS [12]	IRAS [25]	IRAS [60]	IRAS [100]	MSX [8.3]	AKARI [9]	AKARI [18]	AKARI [65]	AKARI [90]	AKARI [140]	AKARI [160]
KW97 14-24	-10.289	-10.133	-10.018	-9.997	-8.303	-7.595	-7.416	-7.488	-9.910	-9.000	—	—	—	—	—
KW97 14-52	-10.369	-8.986	-8.756	-8.913	—	—	—	—	—	-10.304	—	—	—	—	—
IRAS 03243+5819	-11.229	-10.069	-9.965	-9.819	-9.770	-10.620	—	—	-9.726	-9.176	-10.349	—	—	—	—
LkHalphi 272	-10.249	-9.580	-9.489	-9.577	—	-10.213	-10.000	-9.620	—	-10.199	-10.264	—	—	—	—
XY Per	-8.809	-8.480	-8.462	-8.486	-9.017	-9.312	-9.610	-9.653	—	-8.843	-9.246	-9.738	-9.837	-9.943	—
Gahm 21	-10.433	-10.321	-10.160	-10.237	—	—	—	-9.155	—	—	—	—	—	—	—
KW9716 55	-10.289	-9.875	-9.901	-10.056	—	-10.506	-9.602	—	—	—	—	—	—	—	—
OS Per	—	-9.594	-9.605	-9.829	-10.125	-9.444	—	—	—	—	—	—	—	—	—
V347 Aur	-10.405	-9.378	-9.225	-9.273	-9.385	-9.313	-9.342	-9.324	—	-9.548	-9.519	-9.569	-9.578	-9.731	-9.897

**Table 3.** The values of  $\log \lambda F_\lambda$  for the suspected YSOs in passbands of the GSC 2.3.2, 2MASS and Spitzer surveys.

SL	$F$ [0.71]	$J$ [1.26]	$H$ [1.6]	$K_s$ [2.2]	Spitzer [3.6]	Spitzer [4.5]	Spitzer [5.8]	Spitzer [8.0]	Spitzer [24.0]
18	-12.085	-11.038	-10.764	-10.689	-10.679	-10.801	-11.006	-11.308	-12.061
20	–	-11.410	-10.764	-10.413	-10.235	-10.277	-10.286	-10.292	-10.221
30	–	-11.458	-11.036	-10.945	-10.903	-10.977	-11.190	-11.264	–
31	–	-11.238	-10.812	-10.589	-10.355	-10.397	-10.530	-10.552	-10.665
37	-10.253	-9.298	-9.136	-9.081	-10.239	-10.329	-10.638	-10.896	-11.633
51	-12.421	-11.314	-10.968	-10.897	-10.915	-11.009	-11.026	-11.084	-11.301
52	–	-11.102	-9.960	-9.401	-9.115	-9.077	-9.062	–	–
53	-12.293	-11.286	-11.032	-10.937	-10.931	-11.033	-11.126	-11.092	-11.425
54	-11.809	-9.870	-9.276	-8.945	-8.851	-8.853	-8.830	-8.856	–
55	-11.229	-10.682	-10.540	-10.481	-10.611	-10.741	-10.846	-10.864	-10.741
56	–	-10.518	-9.372	-8.669	-8.763	-8.673	-8.082	–	–
57	-12.869	-11.222	-10.920	-10.845	-11.059	-11.041	-11.054	-11.004	-11.337
59	-11.957	-11.262	-10.952	-10.889	-11.019	-11.141	-11.310	-11.444	-11.597
60	-11.717	-10.618	-10.304	-10.229	-10.191	-10.225	-10.234	-10.252	-10.513
61	–	-11.170	-10.460	-10.141	-10.039	-10.021	-10.078	-10.096	-10.289
62	-12.557	-11.046	-10.820	-10.761	-10.571	-10.493	-10.442	-10.268	-10.041
64	-12.945	-10.938	-10.512	-10.385	-10.447	-10.565	-10.646	-10.592	-10.881
65	-12.381	-11.314	-10.872	-10.685	-10.591	-10.573	-10.670	-10.644	-10.689
66	–	-11.578	-10.864	-10.601	-10.511	-10.509	–	–	–
69	–	-10.918	-10.432	-10.209	-10.235	-10.213	-10.170	-10.000	–
70	–	-11.026	-10.480	-10.289	-10.223	-10.269	-10.374	-10.496	–
71	–	-11.110	-10.916	-10.789	-10.519	-10.453	-10.382	-10.080	–
72	–	-11.138	-10.372	-10.145	-10.315	-10.433	-10.578	-10.528	–
74	-12.501	-11.230	-10.832	-10.745	-10.507	-10.473	-10.494	-10.516	–
75	-10.601	-10.086	-9.720	-9.581	-9.535	-9.601	-9.706	-9.720	–
80	–	-10.522	-10.048	-9.857	-9.319	-9.105	-8.870	-8.692	–
89	-12.593	-10.838	-10.460	-10.409	-10.447	-10.389	-10.370	-10.316	-9.981
91	–	-11.538	-11.156	-11.081	-11.131	-11.229	-11.406	-11.624	-12.085
93	–	-11.442	-10.904	-10.793	-10.891	-10.969	-11.066	-11.132	-11.213
94	-12.225	-10.774	-10.340	-10.161	-9.971	-9.977	-10.062	-10.148	-10.325
96	–	-11.394	-10.892	-10.753	-10.611	-10.649	-10.742	-10.784	-10.761
97	–	-11.330	-10.904	-10.849	-10.891	-11.005	-11.178	-11.372	-11.805
145	–	-11.514	-11.188	-11.185	-11.387	-11.505	-11.682	-11.896	-12.309
146	-12.445	-10.970	-10.692	-10.725	-10.855	-11.009	-11.170	-11.224	-11.245
147	–	-11.290	-10.928	-10.929	-11.035	-11.105	-11.210	-11.296	-11.845
148	-12.593	-11.242	-10.972	-11.001	-11.107	-11.241	-11.374	-11.380	-11.469
149	–	-11.582	-11.260	-11.285	-11.523	-11.625	-11.798	-11.976	–

However, SEDs of dusty spiral galaxies in the mid- and far-infrared are quite similar to SEDs of Stage I YSOs (Devriendt et al. 1999; Dale & Helou 2002; Sajina et al. 2006). This is especially true for heavily reddened and redshifted galaxies. Their identification applying the SEDs with only a few infrared photometric points is quite problematic – high resolution optical imaging and infrared spectroscopy are essential (see Luhmann et al. 2006; Rebull et al. 2010).

A few galaxies in our region, identified via the Simbad database, were excluded during the compilation of lists of possible YSOs in Papers II and III. Now we checked for galaxies and extended infrared objects in the 2MASX Database (Skrutskie et al. 2006), NASA/IPAC Extragalactic Database NED (2010) and the Sloan Digital Sky Survey (SDSS) 7th data release (Abazajian et al. 2009). Also, the objects

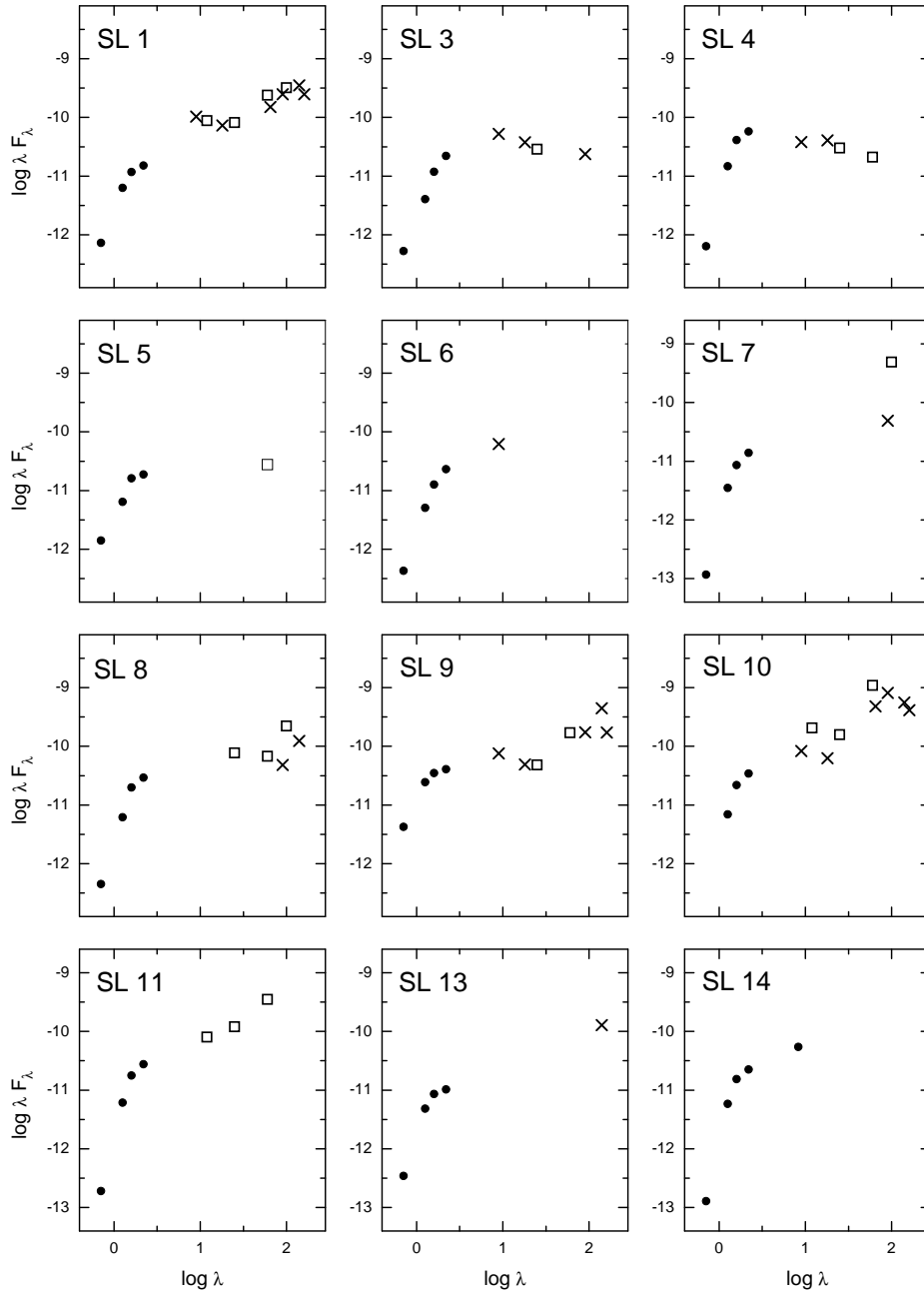


**Fig. 1.** Spectral energy distributions of the suspected YSOs. Dots represent the results for  $R$ ,  $J$ ,  $H$ ,  $K_s$  and MSX passbands, circles are for the Spitzer passbands, squares for the IRAS passbands and crosses for the AKARI passbands.

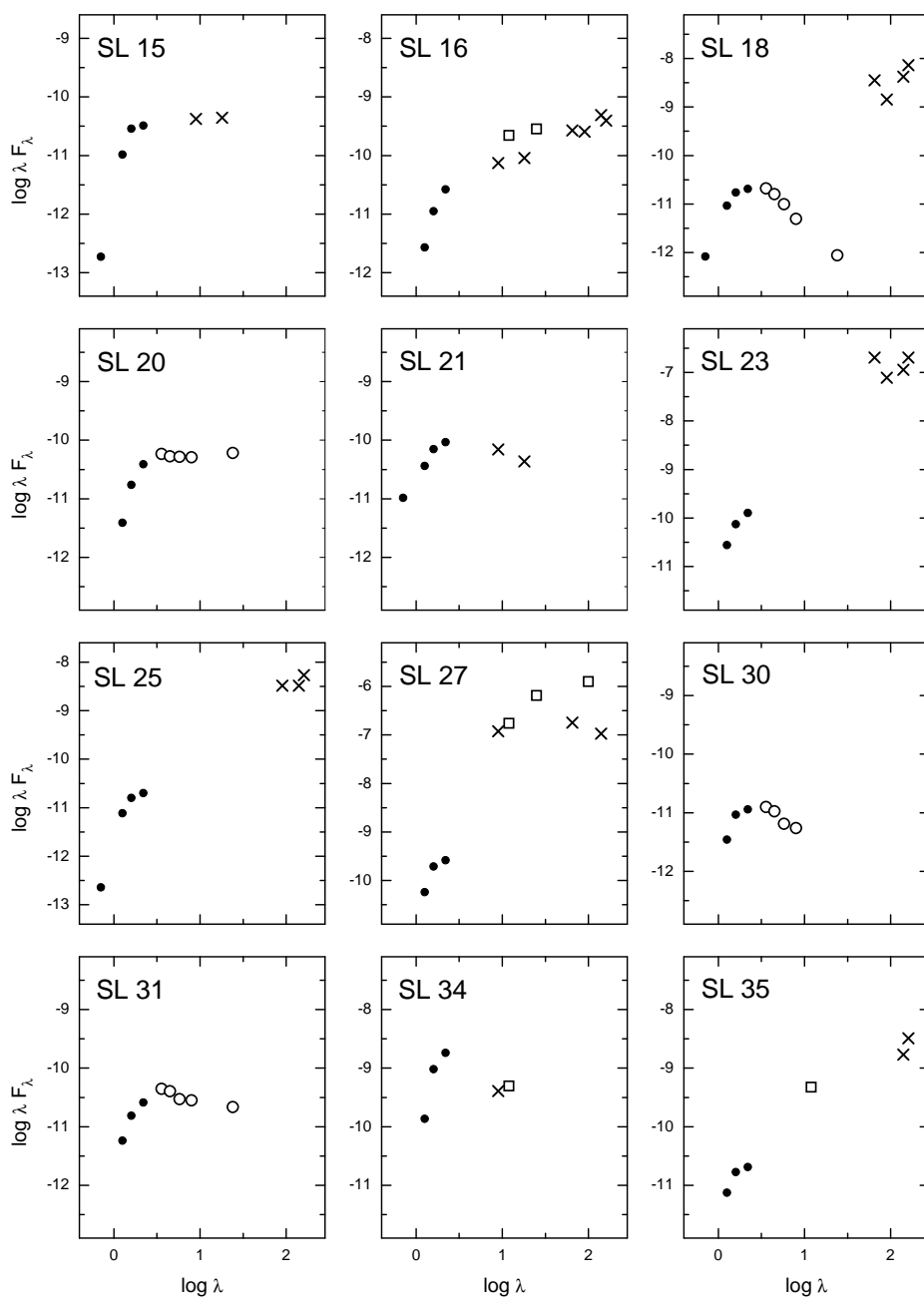


Fig. 1. Continued

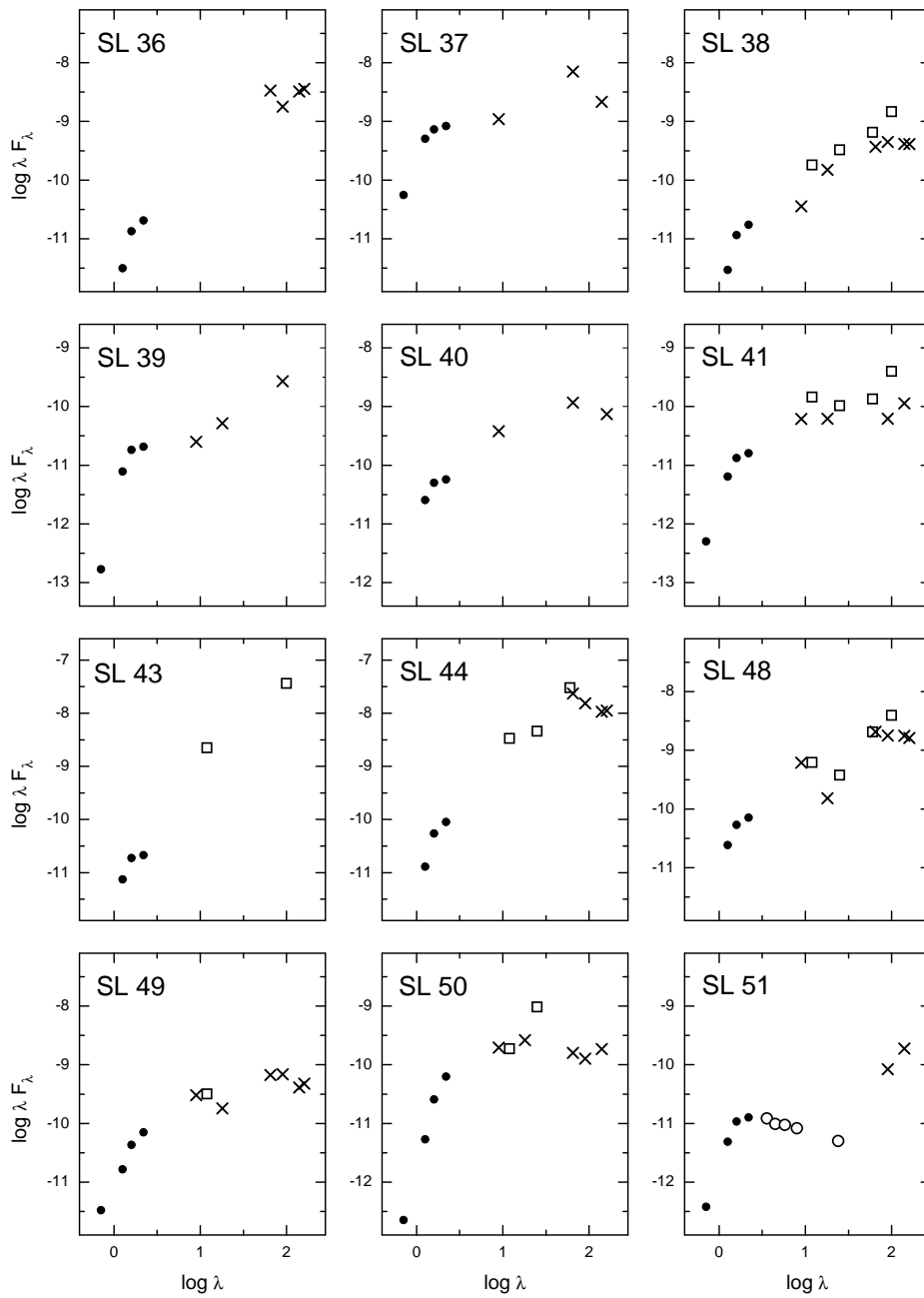


Fig. 1. Continued



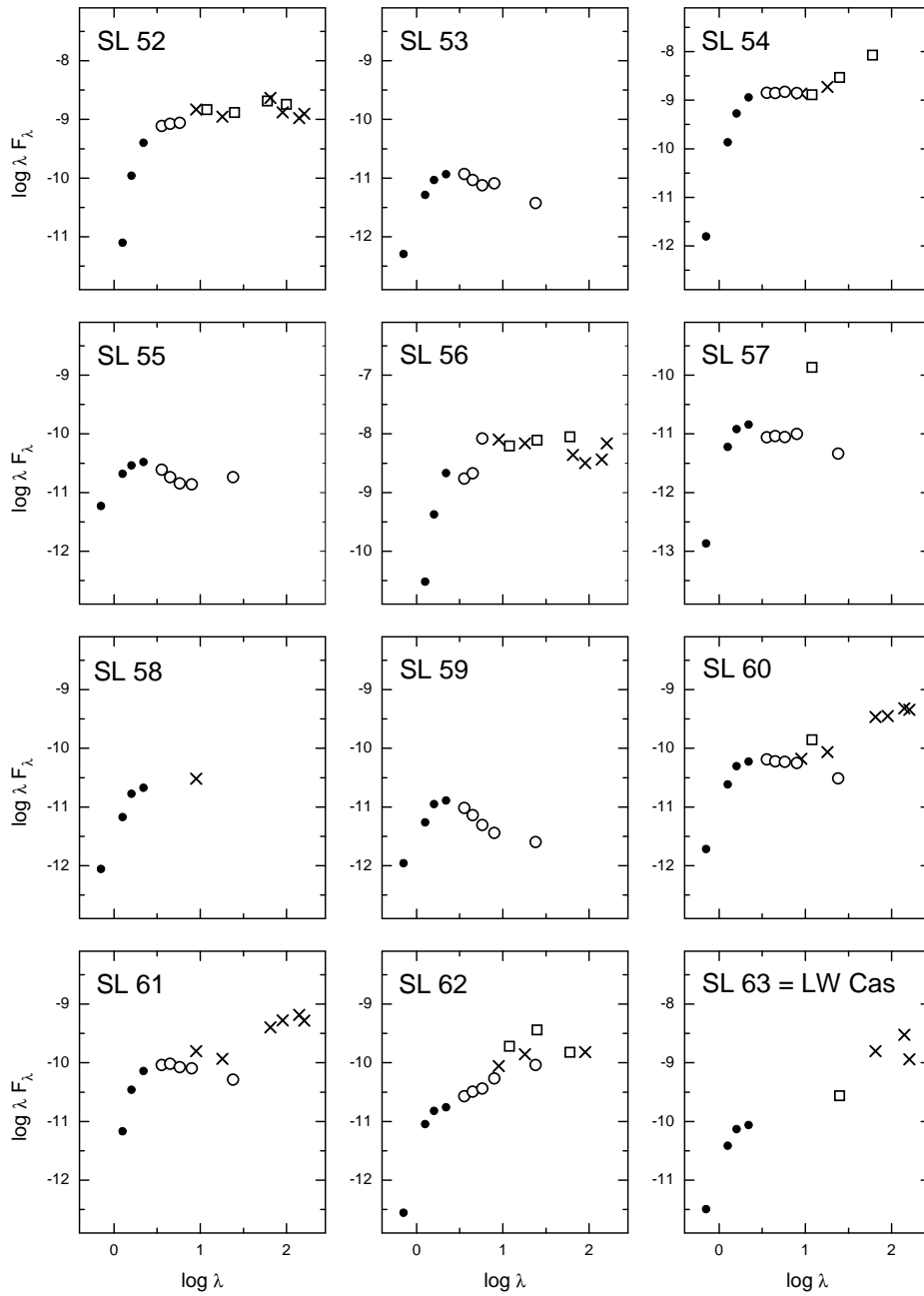


Fig. 1. Continued

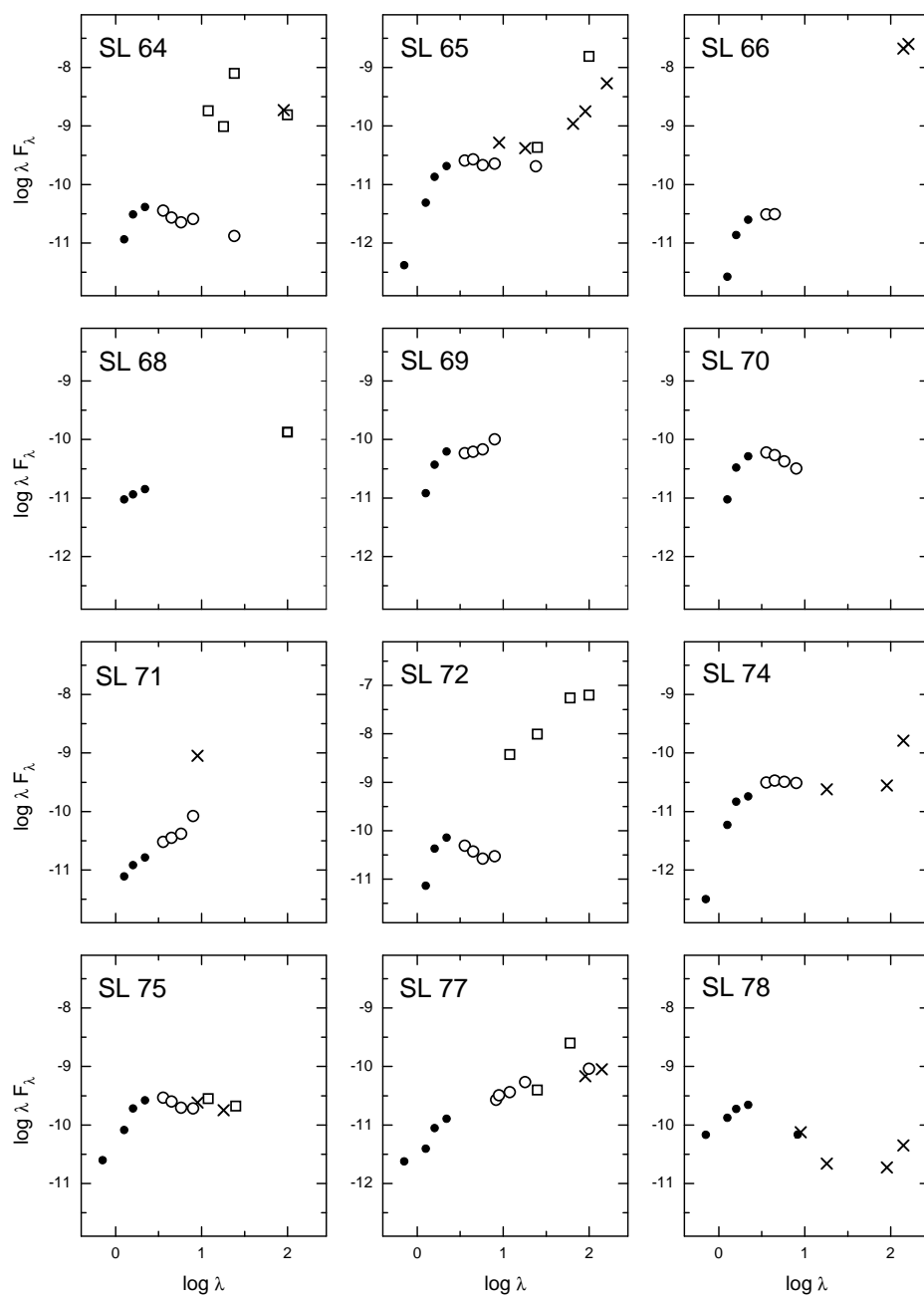


Fig. 1. Continued

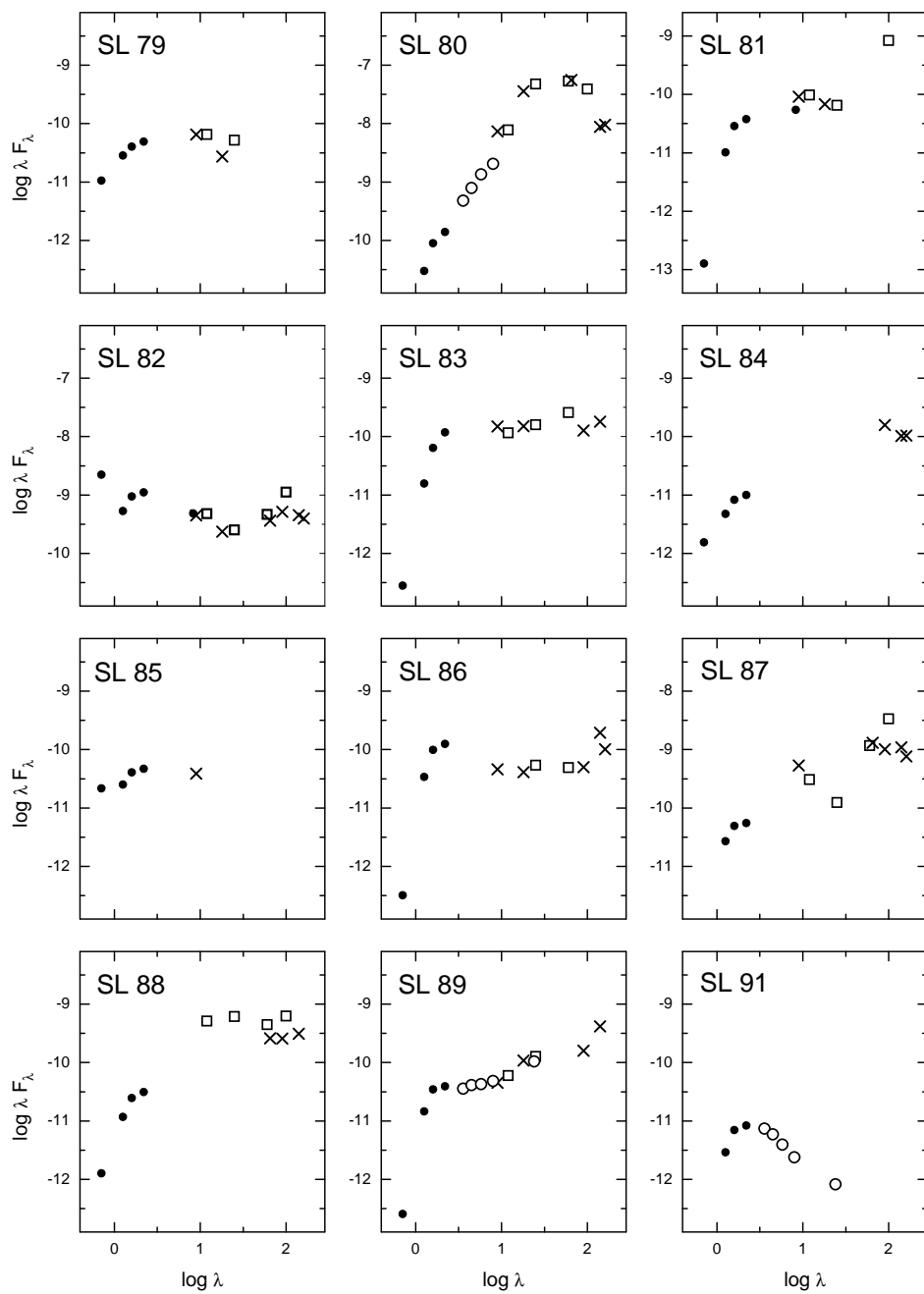


Fig. 1. Continued

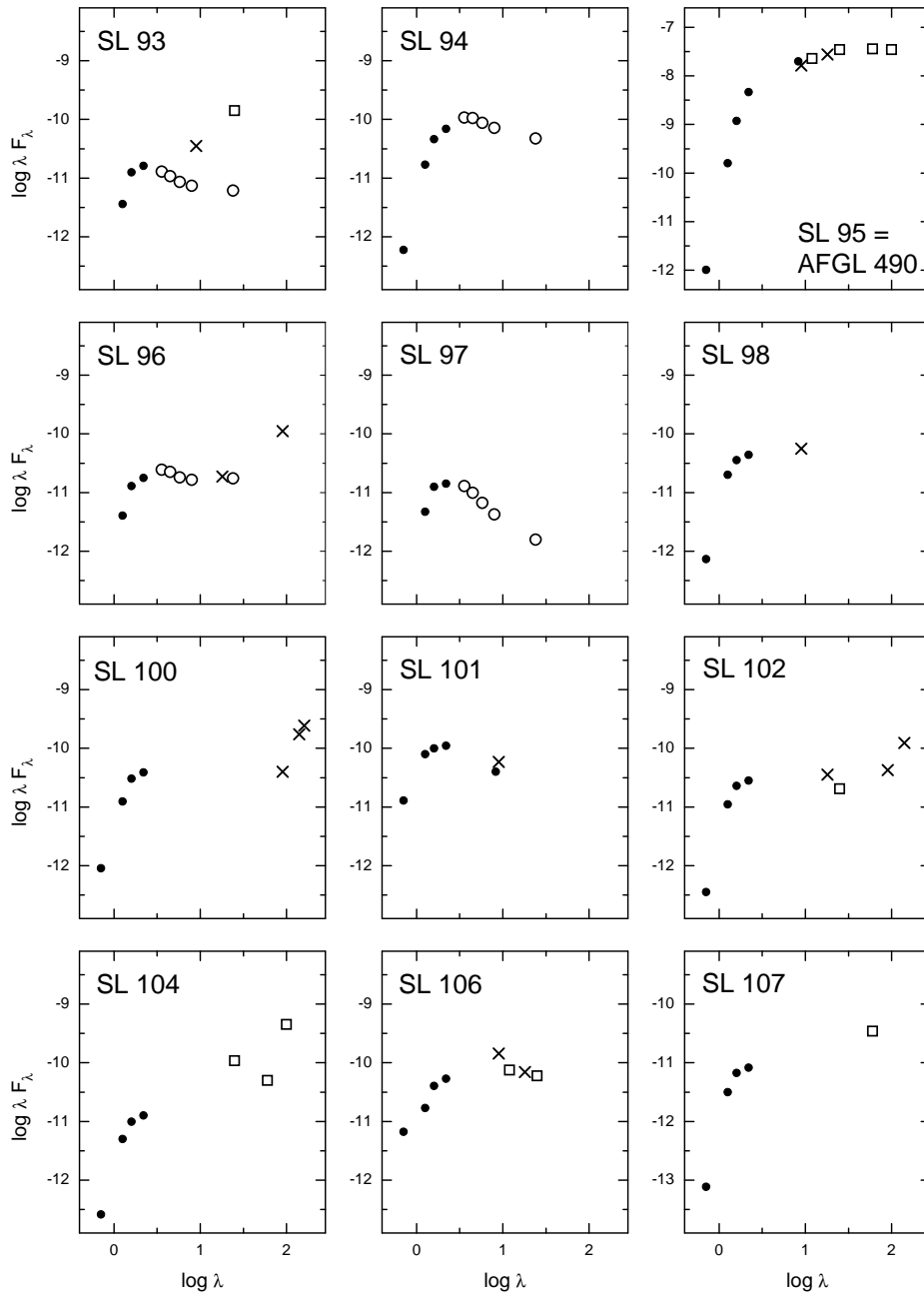


Fig. 1. Continued

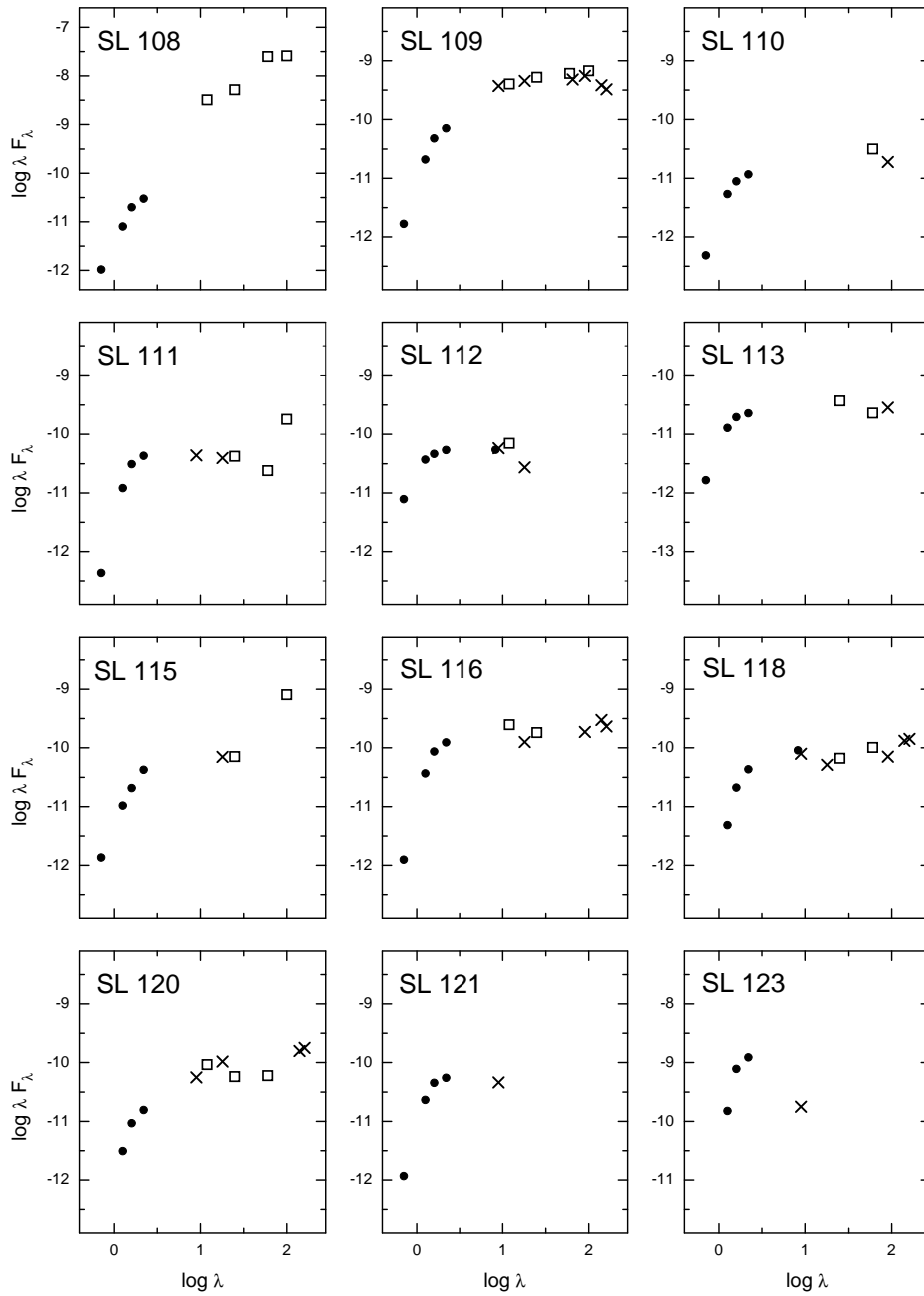


Fig. 1. Continued

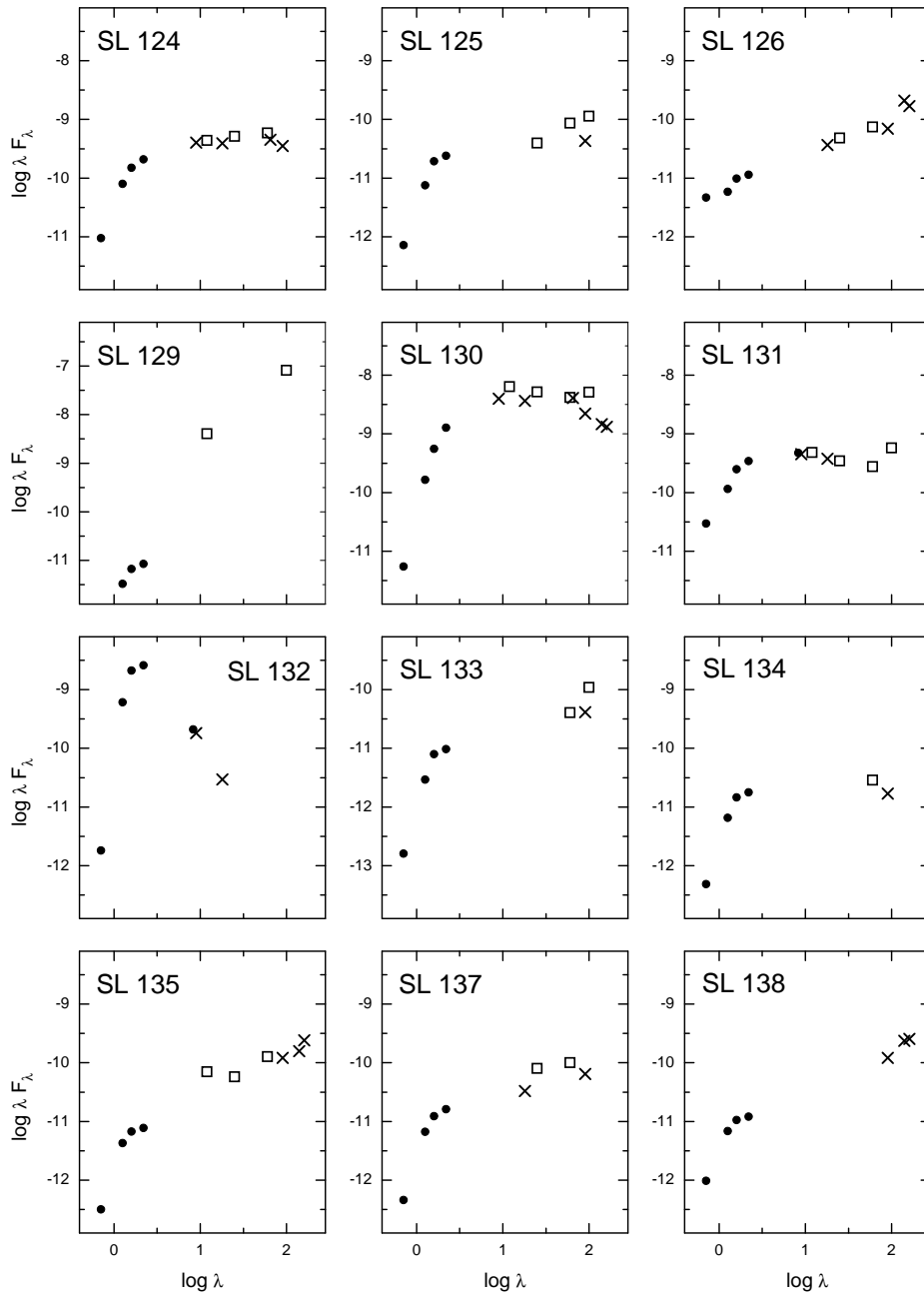


Fig. 1. Continued

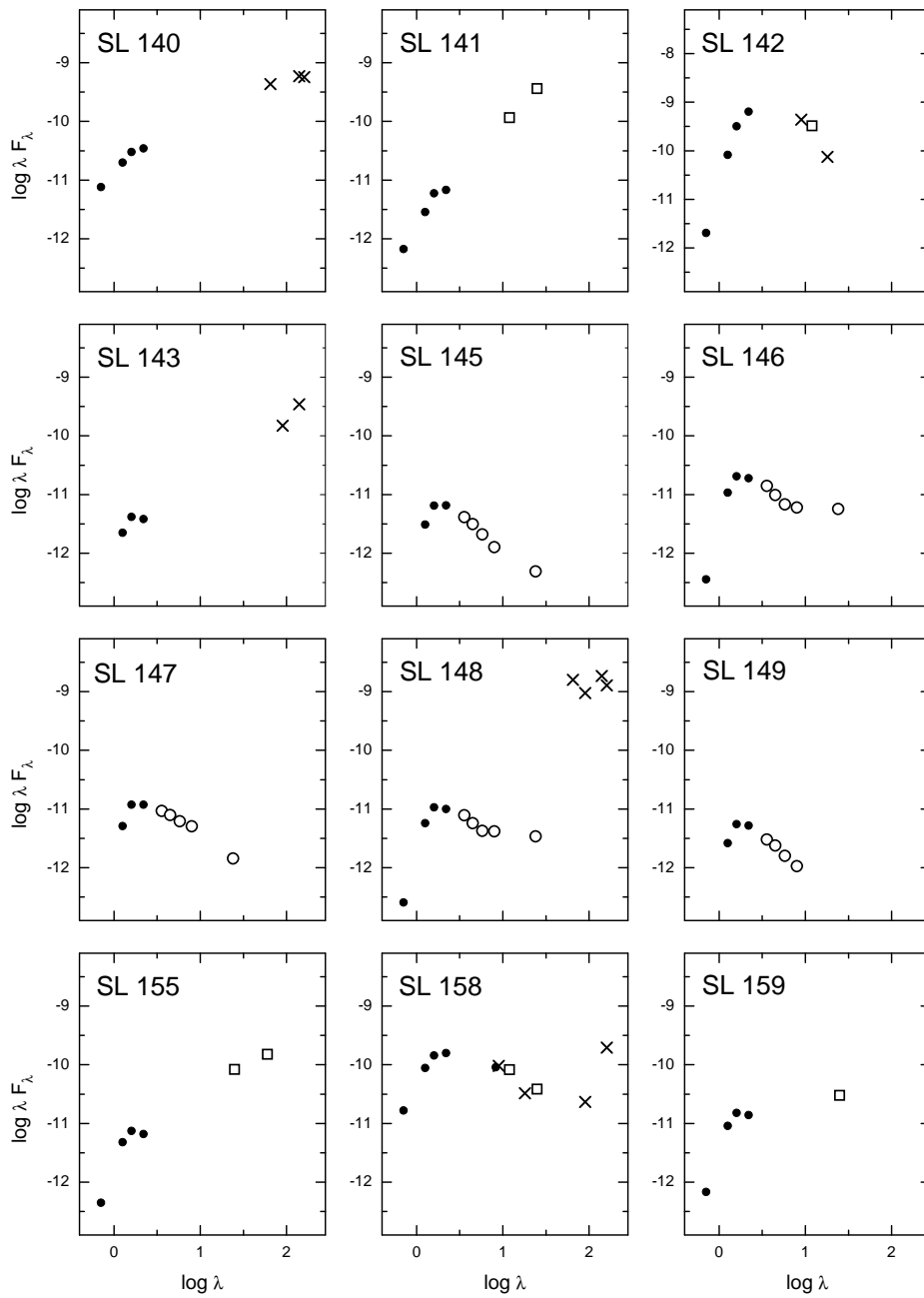


Fig. 1. Continued

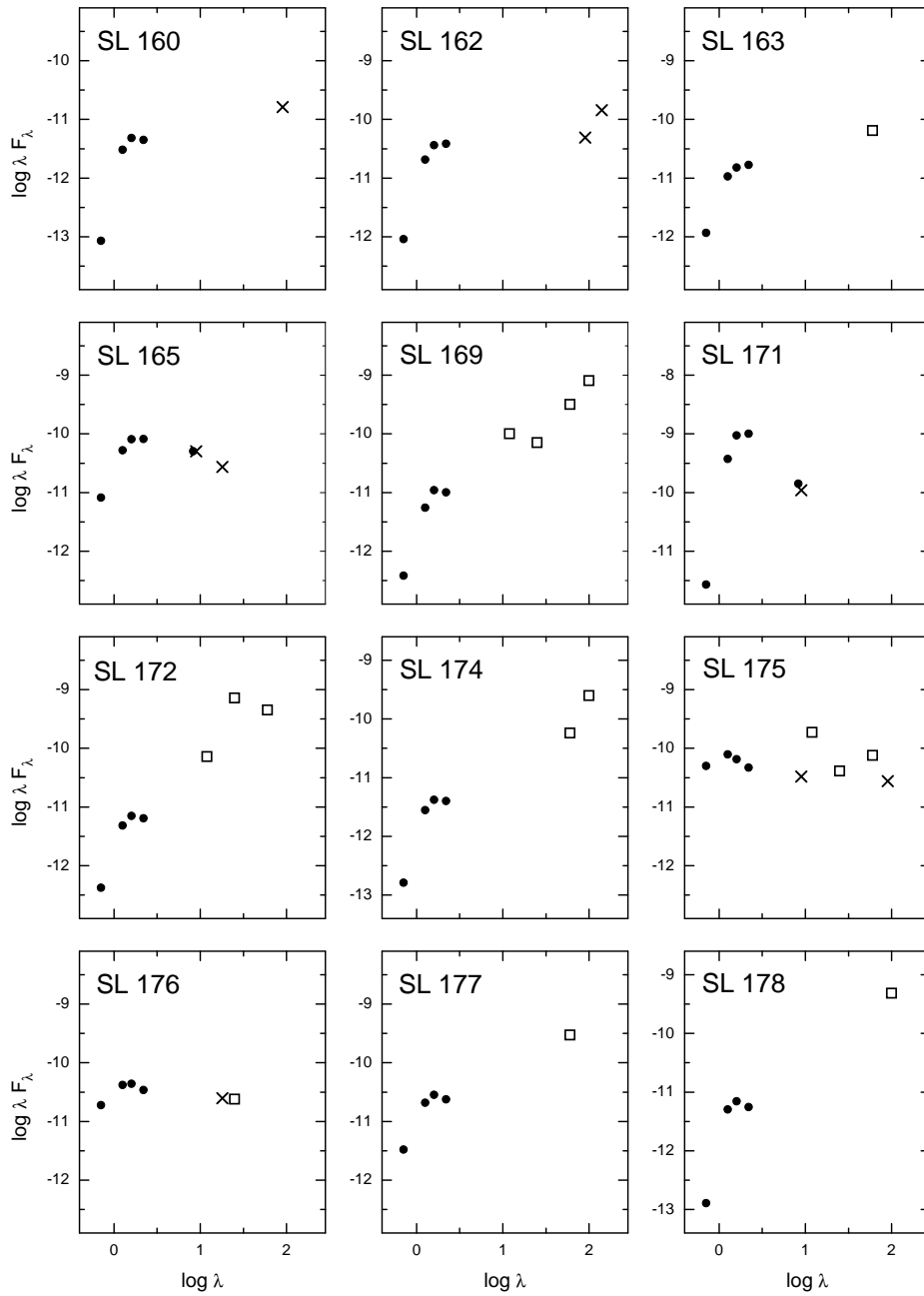


Fig. 1. Continued



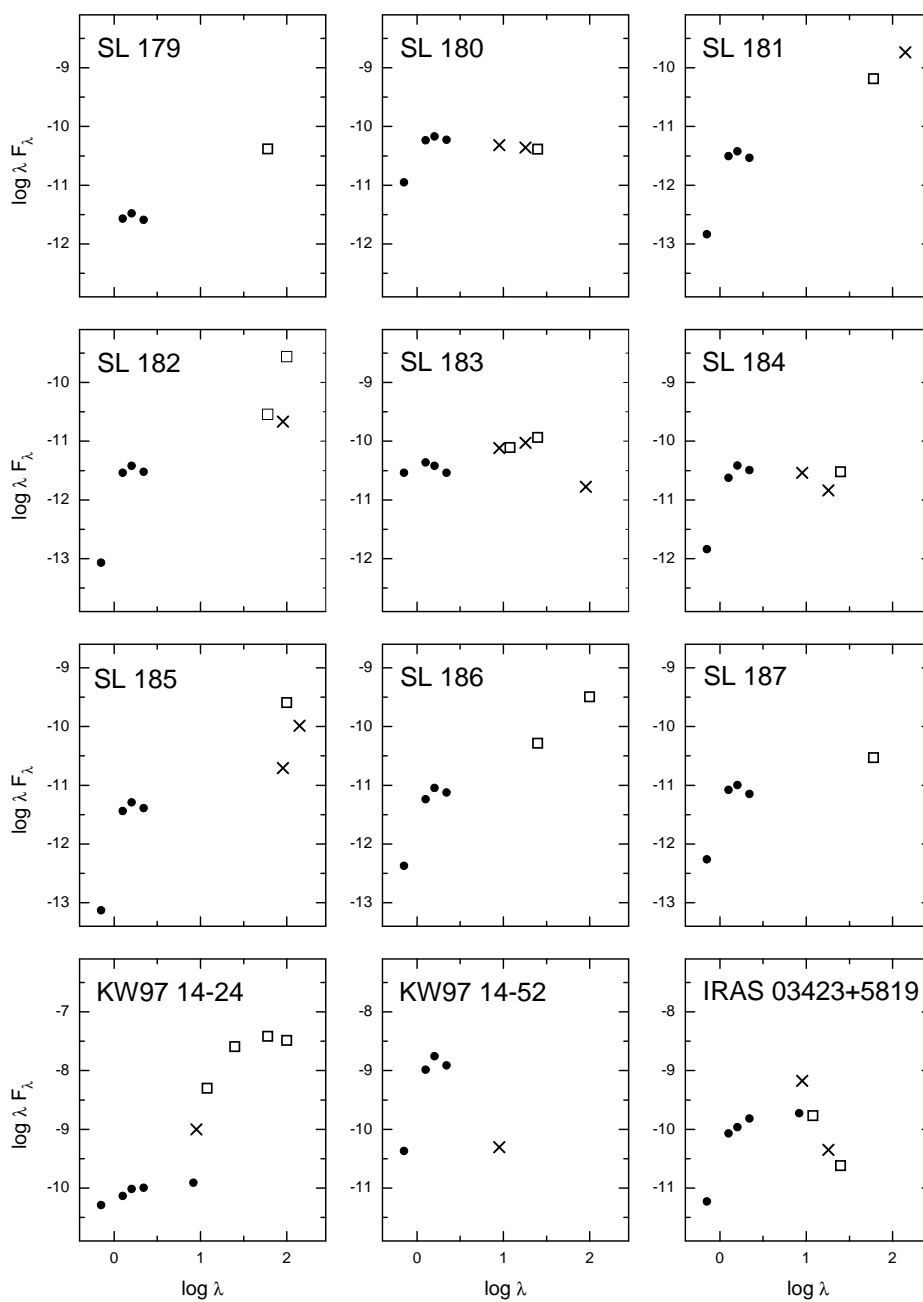
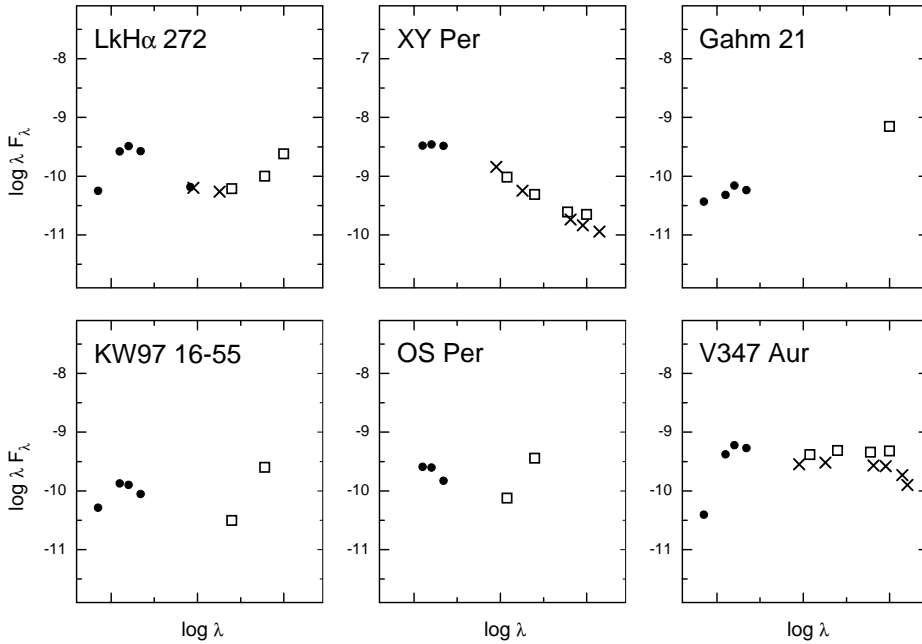


Fig. 1. Continued



**Fig. 1.** Continued

were inspected in the blue, red and infrared images of DSS2 given in the Internet's Virtual Telescope SkyView. The results are described in the following section.

According to Pollo et al. (2010), stars and galaxies can be separated using some flux vs. color and color vs. color diagrams constructed only from the AKARI FIS fluxes. However, their method cannot be applied in our case since for most of the SL objects reliable fluxes are available not in all FIS passbands.

A part of the extended objects discovered by infrared imaging may be so-called ultracompact H II regions, the newly born massive stars hidden in dense dust cocoons (Churchwell 2002). SEDs of these objects rise steeply with increasing  $\lambda$  and have their intensity maxima at  $100 \mu\text{m}$ .

In Figure 2 we show the  $J-H$  vs.  $H-K_s$  diagram for SL objects from Table 1: dots denote YSOs without extended sources, circles denote 19 YSOs with a nearby extended infrared source and crosses denote 14 YSOs with a nearby galaxy. It is evident that all the three types of YSOs do not show significant differences in their location. This means that either the radiation from the extended sources is relatively faint shortward of  $2.5 \mu\text{m}$  or its effect is similar to that of the interstellar and circumstellar reddening. The concentration of points at  $H-K_s = 1.0$  is the selection effect originating from a search for YSOs in Paper II.

#### 4. DISCUSSION

In this section we describe SEDs of the SL objects belonging to different star-forming regions or dust/molecular clouds.

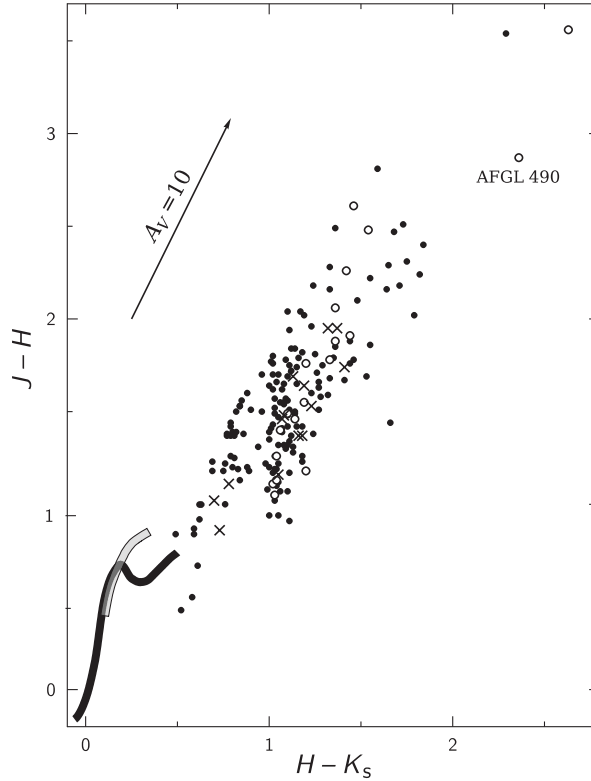


**Fig. 2.** The  $J-H$  vs.  $H-K_s$  diagram for the verified YSOs. Dots denote objects without extended sources, circles denote objects with nearby extended infrared sources and crosses denote objects with nearby galaxies. The black and grey curves denote the main sequence and G8-K-M giants, respectively.

#### 4.1. Objects in W3A (IC 1795) and the dust cloud TGU 879

This group contains the following SL objects: 7, 9, 10, 11, 13, 15, 16, 18, 20, 21, 23, 25, 27, 30, 31, 34, 35, 36, 37, 38, 39. Most of these are located in the W3A (IC 1795) H II region, some are seen in the direction of the dust cloud TGU 879 located south of it. Both the H II region and the dust cloud belong to the Perseus arm (see Paper II). Some of these objects were discovered as YSOs and discussed by Elmegreen (1980), Kerton et al. (2001) and Kerton & Brunt (2003). Most of these objects exhibit SEDs typical for Class I YSOs. The objects SL 15, 20, 21 and 31 may belong to Class II and SL 18, 30, 34 and, possibly, 37 to Class III. The data for the object AKARI-FIS-V1 J0224555+620941, located at  $25.6''$  from SL 18, contradict the Spitzer data and may belong to a different object. A similar situation is with the object AKARI-FIS-V1 J0227184+620030 at  $26.8''$  from SL 37. The SEDs of some of the objects are extremely steep (SL 23, 25, 27, 35 and 36). This should be an indication of heavy interstellar and circumstellar reddening which makes the magnitudes  $F$ ,  $J$ ,  $H$  and  $K_s$  very faint. This conclusion is also supported by the absence of  $F$  magnitudes for these stars in the DSS2 survey (they are fainter than 20.5 mag). Two of the objects, SL 21 and SL 37, were confirmed as YSOs in Paper IV, their spectral types are G0e and

A5e. According to 2MASX, the object SL 10 at a distance of 0.2' has a galaxy. Two extended 2MASX objects are located at SL 23 (0.7') and at SL 37 (0.4').

#### 4.2. Objects in the dust cloud TGU 878 near SU Cas

Six SL objects (Nos. 3, 4, 5, 6, 8 and 14) are located in the dust cloud TGU 878 at  $\ell \approx 132.5^\circ$ ,  $b \approx +9^\circ$ , belonging to the Cam OB1 association located at a distance of 900 pc. The same cloud contains the cepheid SU Cas. The SEDs of the suspected YSOs are of Classes I and II. The object SL 8 = IRAS 02470+6901 according to NED may be a galaxy.

#### 4.3. Objects in W4

Five SL objects, Nos. 40, 41, 43, 44 and 48, are projected on the W4 H II region of the Perseus arm. However, SL 40, according to 2MASX, can be a galaxy centered at 0.3'. SL 44 = IRAS 02245+6115 at 0.2' and SL 48 = IRAS 02327+6019 at 0.4' have extended 2MASX sources which might be related to the infrared clusters identified by Bica et al. (2003a).

#### 4.4. Objects near W5

This group is located in the dust clouds TGU 879 and TGU 912 along the northern edge of the W5 nebula and contains 22 SL objects from Figure 1: 50, 51, 52, 53, 54, 55, 56, 57, 59, 60, 61, 62, 63, 64, 65, 66, 69, 70, 71, 72, 74 and 75. Some of these objects were identified by Carpenter et al. (2000), Kerton & Brunt (2003), Karr & Martin (2003a,b), Bica et al. (2003a,b). The SEDs of these objects are consistent with YSOs of Classes I and II. The objects SL 55, 56, 57, 60, 63, 64, 66, 69, 70, 71 and 72 have extended counterparts at distances 0.2' to 1' listed in 2MASX. Two of them, counterparts of SL 57 and 60, are galaxies. For the object SL 64, the Spitzer and IRAS/AKARI data are in disagreement. The star SL 63 is a known pre-main-sequence variable, LW Cas, of type INA and spectral class A0. In Paper IV the object SL 75 was investigated spectroscopically and recognized as a T Tauri type star of spectral class G0e with strong emissions in H $\alpha$ , O I and Ca II lines. One more YSO, KW97 14-24, which is also located near the edge of W5, was investigated in Paper IV and found to be of spectral class G5e with H $\alpha$  of  $EW = -20.6 \text{ \AA}$ . Nakano et al. (2008) for this star find a similar value,  $EW = -19.4 \text{ \AA}$ . The SED curve of this object is shown in Figure 1 (page 25).

#### 4.5. Objects in LBN 140.07+1.64

Five SL objects, Nos. 79, 80, 83, 84 and 86, are located in the direction of the faint nebula LBN 140.07+1.64 in the Perseus arm, south of Sh 2-202 which is much closer to the Sun. The object SL 80 is known as one of YSOs in the infrared cluster AFGL 437. Other objects were identified by Kerton & Brunt (2003), Karr & Martin (2003a,b) and Bica et al. (2003a). If these objects are pre-main-sequence stars, their SEDs agree with Class II. The spectrum of SL 79 gives spectral type G0e, with strong emissions in H $\alpha$ , O I and Ca II (Paper IV). The emission in H $\alpha$  was also found in the IPHAS survey (Witham et al. 2008). SL 80 = AFGL 437S was classified as an object of Class I based on the Spitzer/IRAC data (Kumar Dewangan & Anandarao 2010). The SED of SL 80 in Figure 1 shows some disagreement between the 2MASS + Spitzer and AKARI data. Probably the AKARI data are affected by other members of the AFGL 437 cluster.

#### 4.6. Objects in Sh 2-202

The faint nebula Sh 2-202, belonging to the Cam OB1 SFR, overlaps several smaller emission features in the Perseus arm (Karr & Martin 2003a). In this direction, two of our objects, SL 81 and SL 82, are seen. The spectrum of SL 82 gives the spectral type G5e, with strong emission in  $H\alpha$  (Paper IV). The object is also known as IRAS 03134+5958 and CPM7 (Campbell et al. 1989). The object is included in the catalog of emission-line stars of the Orion population by Herbig & Bell (1988). The SED of this object is rather peculiar.

#### 4.7. Objects in the dust cloud TGU 942 in the vicinity of AFGL 490

In Papers II and III, 60 possible YSOs were identified in the area of  $3^\circ \times 3^\circ$  with the center at  $\ell = 142.5^\circ$ ,  $b = +1.0^\circ$ , covering the densest part of the dust cloud TGU 942. The SEDs for 39 of them are shown in Figure 1. Their SL numbers are from 89 to 102, 107 and from 143 to 187. We shall describe their properties, distributing them into three groups according to their  $H-K_s$  values.

The group of 12 objects with  $H-K_s \geq 1.0$ , SL numbers between 89 and 107. The objects SL 89, 95, 100 and 107 belong to Class I. The objects SL 93, 94, 96, 98, 101 and 102 belong to Class II. The objects SL 91 and 97 are of Class III. The object SL 95 = AFGL 490 is one of the well known YSOs of Class I, a protostar of spectral class B. Its spectrum was described in Paper IV, together with the spectrum of SL 101 of spectral class G0e. Both objects have strong emissions in  $H\alpha$ , O I and Ca II lines. One more YSO, IRAS 03243+5819 = 2MASS J03281460+5829374, located  $20'$  from AFGL 490, was classified in Paper IV as A-type star with  $H\alpha$  line filled by emission. It shows a peculiar SED (see Figure 1, p. 25). The object SL 103, not present in Figure 1, was found to be a  $H\alpha$  emission star in the IPHAS survey. According to 2MASX, the object SL 94 has an extended infrared source at a distance of  $0.4'$ .

The group of 17 objects with  $H-K_s$  between 0.75 and 1.00, SL numbers between 143 and 174. The objects SL 143, 155, 160, 163, 169, 172 and 174 belong to Class I, SL 146, 148, 158, 159, 162, 165 to Class II, and SL 145, 147, 149, 171 to Class III. For SL 148, the data from Spitzer and AKARI are in obvious contradiction. Probably the 2MASS+Spitzer object and the AKARI object, separated by  $28''$ , are different objects. The objects SL 158 (A0e), SL 163 (F:e) and SL 165 (G5e) were investigated spectroscopically (Papers IV and V). The spectra of two more stars of this group, SL 144 (G0e) and SL 153 (F0e), were obtained (Paper V), but no infrared data for these objects are available. In SL 161,  $H\alpha$  emission was found by the IPHAS survey. For the objects SL 169 and SL 174, the identification with the IRAS sources is doubtful ( $> 1'$ ). According to 2MASX, a small galaxy is located at  $0.4'$  from SL 172.

The group of 13 objects with  $H-K_s$  between 0.50 and 0.75, SL numbers between 175 and 187. The objects SL 177, 178, 179, 181, 182, 185, 186 and 187 belong to Class I. The objects SL 175, 176, 180, 183 and 184 belong to Class II. In Paper V the spectra for the following objects were investigated: SL 175 (F0e), SL 176 (G0e), SL 177 (A2e), SL 183 (A2e), SL 184 (F:e). In SL 177,  $H\alpha$  emission was found by the IPHAS survey. For the objects SL 175 and SL 185, the IRAS identification is doubtful ( $> 1'$ ).

#### 4.8. Objects in the remaining part of the dust cloud TGU 942

Figure 1 contains eight more objects in the TGU 942 cloud scattered over nearly

$3^\circ$  along the Galactic longitude. Most of these objects are projected on the molecular clouds of the Perseus arm (see Paper II). Four SL objects (104, 105, 106 and 108) are located in the faint emission nebula Sh 2-203 and belong to the infrared cluster BDSB 59 (Bica et al. 2003b). The SEDs of three of these objects are shown in Figure 1. According to the 2MASX catalog, SL 106 is only by  $0.4'$  from a galaxy. The object SL 109 is the well-known Class I YSO CPM 8 (Campbell et al. 1989). The remaining four objects, SL 110, 111, 112 and 113 are likely to be YSOs of Class II.

#### 4.9. Objects in the vicinity of the Sh 2-205 emission nebula

Four SL objects are located close to the H II region Sh 2-205. The SEDs of two of them, SL 115 and SL 116, are shown in Figure 1: both seem to be of Class II. Probably the stars belong to the infrared cluster FSR 655 (Froebrich et al. 2007).  $H\alpha$  emission in SL 116 was found in the IPHAS survey. In the same area, eight emission-line stars discovered by G. Gahm and investigated spectroscopically in Papers IV and V are located. The SED of one of them, Gahm 21 (spectral type Ke), is shown in Figure 1 (p. 26), admitting that IRAS 03561+5123 with the position  $33''$  away is the same object. Other Gahm objects are absent in the IRAS, MSX and AKARI databases.

#### 4.10. Objects within the dust circle centered on the open cluster NGC 1528

In Paper I, a circle of dust clouds with a diameter of  $\sim 8^\circ$ , centered at  $(\ell, b) = (152^\circ, +0.5^\circ)$ , close to the open cluster NGC 1528, was described. Within this circle, Paper II lists 20 SL objects (from SL 118 to SL 137) but only 15 of these have SEDs shown in Figure 1. The objects SL 126, 129, 133, 135 and 137 belong to Class I, objects SL 118, 120, 121, 124, 125, 130, 131 and 134 to Class II and objects SL 123 and 132 to class III. The best known YSO is SL 130 = CPM 12 in the nebula Sh 2-209 (Campbell et al. 1989). Objects SL 123, 129 and 130 may be related to the infrared clusters BDSB 61 and BDSB 65 (Bica et al. 2003b). SL 124 is known as a T Tauri type star (GLMP 49, García-Lario et al. 1997). Objects SL 126 and 137 may be overlapped by images of the nearby galaxies.

Four SL objects, 138, 140, 141 and 142, are located at the extension of dust clouds of the afore-mentioned circle, close to the dust clouds TGU 1045 and TGU 1056. The first three objects exhibit SEDs of Class I and SL 142 of Class III. CO radial velocities show that the object SL 140 belongs to the Perseus arm (Wouterloot & Brand 1989).

#### 4.11. Other objects

SL 1 = IRAS 02081+6225. According to the NED and 2MASX databases this object is a galaxy.

SL 49 = IRAS 02475+6156. By infrared imaging Iwata et al. (1997) find this object to be a possible galaxy.

SL 58. Extended source in the DSS2 blue, red and infrared images; a possible galaxy.

SL 68 = IRAS 03074+6211. Extended or binary source in DSS2 blue, red and infrared images.

SL 77 and 78. These two objects, separated by  $3.2'$ , are located in the direction of the dark cloud TGU 931 which belongs to dust layer of the Cam OB1 association. SL 77 = 2MASS J02512410+5542038 can be related to IRAS 02476+5529 at  $72''$  or

AKARI-FIS-V1 J0251208+554217 at  $31''$ . In the IPHAS survey it is recognized as a  $H\alpha$  emission star. The object SL 78 = 2MASS J02514696+5542014 was classified as F5e in Paper IV. If it is related to the object AKARI-FIS-V1 J0251409+554223 at a distance of  $56''$ , the YSO should belong to Class II.

SL 85 = 2MASS J03300237+6125473. The object is seen in the direction free of dark clouds. Another object (2MASS J03300208+6125565) of oblong shape and with similar brightness in the red and near infrared is located at  $9''$  north. This second object is fainter than SL 85 both in the blue and in the  $J$ ,  $H$ ,  $K_s$  magnitudes. The AKARI-IRC-V1 J0330022+612547 flux at  $9\ \mu\text{m}$  is available. The objects may be extragalactic.

SL 87 and SL 88. These two objects of Class I are located in the southern branch of the dark cloud TGU 942 towards the small emission nebula LBN 140.77-1.42 (Karr & Martin 2003a) in the Perseus arm.  $H\alpha$  emission in the spectrum of SL 88 was found by the IPHAS survey.

## 5. CONCLUSIONS

In the previous papers in this series (Papers II and III), 187 objects (designated as SL objects) located in the Milky Way between Galactic longitudes  $132\text{--}158^\circ$  and latitudes  $\pm 12^\circ$ , were suspected as pre-main-sequence stars or YSOs on the grounds of their 2MASS, IRAS and MSX infrared colors. The Spitzer and AKARI data release gave us the possibility to construct infrared spectral energy distributions for more objects and to verify their evolutionary status. In this study we constructed the SEDs between  $0.7\ \mu\text{m}$  and  $160\ \mu\text{m}$  for 141 objects of our sample, taking the data from the GSC 2.3.2, 2MASS, IRAS, MSX, Spitzer and AKARI catalogs. The analysis of the SEDs of these objects, combined with their surface distribution, leads to the conclusion that about 45%, 41% and 14% of them can be YSOs of Classes I, II and III, respectively. Most of these objects are heavily reddened by interstellar and circumstellar dust what makes them quite faint in the red and near infrared spectral regions. About 30 of SL objects have extended 2MASX sources within  $1'$ , which can affect photometric measurements of the point-like sources. Such extended sources usually are small ionized regions, clusterings of faint infrared stars or galaxies.

Star-forming dusty galaxies contaminate SEDs of YSOs, rising the intensity at  $100\ \mu\text{m}$  due to dust emission. This makes the SED of an YSO similar to that of the Class I object. The presence of a galaxy can be identified either by inspecting optical or near infrared images in the vicinity of YSO or by spectral observations. We identified 13 galaxies in the vicinity of SL objects by inspecting blue, red and infrared images of the DSS2 survey and checking the NED database as well as 2MASX and SDSS catalogs. We cannot exclude that more SEDs remain contaminated by nearby unidentified galaxies.

The concentration of YSOs in close groups, clusters and gas/dust clouds provides an additional statistical criterion for their separation from galaxies. However, the concentration of infrared objects towards dense clouds alone does not mean that we have a group of objects located close to each other in space. As it was shown in Paper III, distant heavily reddened K and M giants also demonstrate a tendency to concentrate in the direction of the densest dust clouds, thus imitating clustering of real YSOs. Therefore, for the identification of embedded groups and clusters of YSOs, photometry in the mid- and far-infrared and spectral observations become essential.

ACKNOWLEDGMENTS. This research includes observations with AKARI, a JAXA project with the participation of ESA. The use of the 2MASS, IRAS, MSX, Spitzer, SkyView and Simbad databases is acknowledged. We are thankful to Stanislava Bartašiūtė, Vygandas Laugalys and Edmundas Meištas for their help preparing the paper.

## REFERENCES

- Abazajian K. N., Adelman-McCarthy J. K., Agueros M. A. et al. 2009, *ApJS*, 182, 543
- Bica E., Dutra C. M., Barbuy B. 2003a, *A&A*, 397, 177
- Bica E., Dutra C. M., Soares J., Barbuy B. 2003b, *A&A*, 404, 223
- Campbell B., Persson S. E., Matthews K. 1989, *AJ*, 98, 643
- Carpenter J. M., Heyer M. H., Snell R. L. 2000, *ApJS*, 130, 381
- Churchwell E. 2002, *ARA&A*, 40, 27
- Corbally C. J., Straizys V. 2008, *Baltic Astronomy*, 17, 21 (Paper IV)
- Corbally C. J., Straizys V. 2009, *Baltic Astronomy*, 18, 1 (Paper V)
- Dale D. A., Helou G. 2002, *ApJ*, 576, 159
- Devriendt J. E. G., Guiderdoni B., Sadat R. 1999, *A&A*, 350, 381
- Dobashi K., Uehara H., Kandori R., Sakurai T., Kaiden M., Umemoto T., Sato F. 2005, *PASJ*, 57, S1
- Elmegreen D. M. 1980, *ApJ*, 240, 846
- Froebrich D., Scholz A., Raftery C. L. 2007, *MNRAS*, 374, 399
- García-Lario P., Manchado A., Pych W., Pottasch S. R. 1997, *A&AS*, 126, 479
- Gutermuth R. A., Megeath S. T., Myers P. C. et al. 2009, *ApJS*, 184, 18
- Herbig G. H., Bell K. R. 1988, *Lick Obs. Bull.*, No. 1111
- Ishihara D., Onaka T., Kataza H. et al. 2010, *The AKARI/IRC Mid-Infrared All-Sky Survey*, *A&A*, 514, A1
- Iwata I., Nakanishi K., Takeuchi T. et al. 1997, *PASJ*, 49, 47
- Karr J. L., Martin P. G. 2003a, *ApJ*, 595, 880
- Karr J. L., Martin P. G. 2003b, *ApJ*, 595, 900
- Kataza H., Alfageme C., Cassatella A. et al. 2010, *AKARI-IRC Point Source Catalogue Release Note, Version 1.0*  
<http://www.ir.isas.jaxa.jp/AKARI/Observation/PSC/Public/>
- Kerton C. R., Brunt C. M. 2003, *A&A*, 399, 1083
- Kerton C. R., Martin P. G., Johnstone D., Ballantyne D. R. 2001, *ApJ*, 552, 601
- Koenig X. P., Allen L. E., Gutermuth R. A. et al. 2008, *ApJ*, 688, 1142
- Kumar Dewangan L., Anandarao B. G. 2010, *MNRAS*, 402, 2583
- Lada C. J. 1987, in *Star Forming Regions* (IAU Symp. 115), eds. M. Peimbert & J. Jugaku, Reidel Publ. Comp., Dordrecht, p. 1
- Lasker B. M., Lattanzi M. G., McLean B. J. et al. 2008, *AJ*, 136, 735; CDS Catalog I/305, version GSC 2.3.2
- Luhmann K. L., Whitney B. A., Meade M. R. et al. 2006, *ApJ*, 647, 1180
- Murakami H., Baba H., Barthel P. et al. 2007, *PASJ*, 59, S369
- Nakano M., Sugitani K., Niwa T. et al. 2008, *PASJ*, 60, 739
- NED, 2010, <http://nedwww.ipac.caltech.edu/>
- Pollo A., Rybka P., Takeuchi T. T. 2010, *A&A*, 514, A3
- Reach W. T., Megeath S. T., Cohen M. et al. 2005, *PASP*, 117, 978



- Rebull L. M., Padgett D. L., McCabe C.-E. et al. 2010, *ApJS*, 186, 259
- Rieke G. H., Blaylock M., Decin L. et al. 2008, *AJ*, 135, 2245
- Robitaille T. P., Whitney B. A., Indebetouw R. et al. 2006, *ApJS*, 167, 256
- Robitaille T. P., Whitney B. A., Indebetouw R., Wood K. 2007, *ApJS*, 169, 328
- Ruch G. T., Jones T. J., Woodward C. E. et al. 2007, *ApJ*, 654, 338
- Sajina A., Scott D., Dennefeld M. et al. 2006, *MNRAS*, 369, 939
- Shirahata M., Matsuura S., Hasegawa S. et al. 2009, *PASJ*, 61, 737
- Skrutskie M. F., Cutri R. M., Stiening R. et al. 2006, *AJ*, 131, 1163 (2MASX catalog)
- Straižys V. 1992, *Multicolor Stellar Photometry*, Pachart Publ. House, Tucson, Arizona (available in pdf format at <http://www.itpa.lt> or <http://www.tfai.vu.lt>)
- Straižys V., Laugalys V. 2007a, *Baltic Astronomy*, 16, 167 (Paper I)
- Straižys V., Laugalys V. 2007b, *Baltic Astronomy*, 16, 327 (Paper II)
- Straižys V., Laugalys V. 2008a, *Baltic Astronomy*, 17, 1 (Paper III)
- Straižys V., Laugalys V. 2008b, *Young Stars and Clouds in Camelopardalis*, in *Handbook of Star Forming Regions, vol. 1. The Northern Sky*, ed. B. Reipurth, ASP, p. 294
- Whitney B. A., Wood K., Bjorkman J. E., Wolff M. J.. 2003a, *ApJ*, 591, 1049
- Whitney B. A., Wood K., Bjorkman J. E., Cohen M. 2003b, *ApJ*, 598, 1079
- Whitney B. A., Indebetouw R., Bjorkman J. E., Wood K. 2004, *ApJ*, 617, 1177
- Witham A. R., Knigge C., Drew J. E. et al. 2008, *MNRAS*, 384, 1277
- Wouterloot J. G. A., Brand J. 1989, *A&AS*, 80, 149
- Yamamura I., Makiuti S., Ikeda N. et al. 2010, *AKARI-FIS Bright Source Catalogue Release Note*, <http://www.ir.isas.jaxa.jp/AKARI/Observation/PSC/Public/>
- Zdanavičius J., Zdanavičius K., Straižys V. 2005, *Baltic Astronomy*, 14, 31